Feature-based Energy Consumption Quantitation Strategy for Additive Manufacturing of Complex Parts

Mengdi Gao (mengdgao@163.com)
Suzhou University
Conghu Liu
Suzhou University
Qingyang Wang
Suzhou University
Lei Li
Hefei University of Technology
Xinyu Li
Hefei University of Technology
Zhilin Ma
Suzhou University
Zhifeng Liu
Hefei University of Technology

Original Article

Keywords: Additive manufacturing, Energy consumption, Feature-based, Complex parts, Typical AM features

Posted Date: October 29th, 2020

DOI: https://doi.org/10.21203/rs.3.rs-96925/v1

Feature-based energy consumption quantitation strategy for additive manufacturing of complex parts

Mengdi Gao[1]*, Conghu Liu[1,2], Qingyang Wang[1], Lei Li [3], Xinyu Li [3], Zhilin Ma[1], Zhifeng Liu[3*]

[1] School of Mechanical and Electronic Engineering, Suzhou University, Suzhou 234000, P. R. China

[2] Tsinghua University School of Economics and Management, Tsinghua University, Beijing 100089, P. R. China

[3] School of Mechanical Engineering, Hefei University of Technology, Hefei 230009, P. R. China

Abstract

Additive manufacturing (AM) has significant advantages over conventional manufacturing technologies, including freedom of design, mass customization, and the ability to produce complex structures. Because reducing manufacturing energy is an essential challenge for industrial sustainability and national economics, the trend toward AM motivates us to explore the energy consumption of AM to address energy efficiency. Existing energy consumption quantitation methods for AM parts require complex models, and the energy consumption characteristics of AM equipment muse be considered in the quantitative analysis process. Therefore, a feature-based energy consumption quantitation method for complex AM parts is proposed that uses a simple model and can be applied to different AM technologies. A feature segmentation method is first proposed to divide complex AM parts into typical AM features (AMFs). Then, the energy consumption model is developed for each AMF to quantify the energy consumption during

[1] Corresponding author: Mengdi Gao(mengdgao@163.com), Tel: +86-15156218446, address: Suzhou University, Anhui Suzhou 234000, P. R. China

fabrication of the entire part. Finally, the energy consumption characteristics of a typical mechanical part manufactured by three different kinds of AM processes—fuse deposition modeling (FDM), stereolithography (SLA), and selective laser melting (SLM)—are investigated using the proposed feature-based energy consumption quantitation method and measured in an experimental case study. The results show that the proposed method can effectively and quickly predict the energy consumption of AM part manufacturing. Moreover, the efficiency of different types of AM processes is compared and discussed to address applicable efficiency improvement methods. This method can predict the energy consumption of complex AM parts, and can be integrated into the AM three-dimensional software model, providing a reference for structural optimization of AM parts.

Keywords: Additive manufacturing; Energy consumption; Feature-based; Complex parts; Typical AM features

1 Introduction

Additive manufacturing (AM) technology has developed rapidly in recent years, and is now a widely used manufacturing process by which any complex digital model can be translated to an entity quickly. The recent growth in AM has increased manufacturing industry return and enhanced industrial competitiveness. China is paying more attention to the development of AM technology. The report “Made in China 2025” states that it is important to accelerate the research and development of AM technology and equipment. Three-dimensional (3D) printing is an important AM technology. According to a research report on the market prospect and investment of the 3D printing industry in 2019, the market scale of China’s 3D printing was 2.36 billion RMB

in 2018, with a growth rate of nearly 42% [1]. In addition, *Wohlers Report 2020* shows that the application proportion of AM technology in the automobile, aerospace, and industrial machinery industries is increasing every year [2].

AM technology can produce parts with complex shapes that cannot be processed by traditional manufacturing technology such as reducing, forging, and casting [3]. Moreover, AM technology improves the machinability of materials that are difficult to process, which greatly expands its application in engineering [4, 5]. However, AM is a large energy consumer because it uses high-energy beams (such as laser beams, electron beams, plasma, etc.), and the manufacturing efficiency is low and the production cycle long because of layer-by-layer stacking. High energy consumption increases the production cost of AM products and causes environmental problems. For example, a large amount of fossil fuel combustion for power generation produces a large amount of greenhouse gas (GHG) emissions (China's GHG emissions are up to 1.03×10^9 t [6]), which increases the greenhouse effect. Therefore, the energy consumption and environmental impact of AM have attracted a great deal of attention [7].

At present, the energy consumption analysis methods for AM can be divided into two categories. One is the direct energy consumption measurement of AM equipment in parts processing. Laser AM is of particular concern for its high energy consumption, and it has been the focus of many developments in this category. Baumers et al. divided the energy consumption of the laser sintering (LS) AM process into job-dependent, time-dependent, geometry-dependent, and z-height–dependent energy consumption, and investigated them through power test experiments [8]. Telenko et al. compared the energy efficiency of selective laser sintering (SLS) and injection molding in the fabrication of nylon parts through experimental tests [9]. Zhu et al. analyzed the

energy consumption and mechanical properties of selective laser melting (SLM) under different process parameters, which can provide a reference for process parameter optimization [10]. Song et al. divided the energy consumption processes of fuse deposition modeling (FDM) into standby period, preheating process, and printing process, and analyzed the energy consumption of these three processes through tests to identify the energy loss caused by human or printer error [11]. Peng et al. analyzed the influence of process parameters on energy consumption and product surface roughness in FDM processing [12]. Ajay et al. measured the energy consumption of FDM and proposed an energy consumption optimization method known as 3DGates [13].

The other method of energy consumption quantitation for AM is energy consumption modeling using the process parameters. Peng established an energy consumption model for FDM by dividing the energy consumption of AM into primary energy consumption and secondary energy consumption [14]. Simon et al. established an energy and material consumption model for the 3D printing process and verified the accuracy of the unit-level process model through experimental data, which was also used a basis for 3D printing lifecycle analysis [15]. Hettesheimer et al. developed an energy consumption model for SLS and compared the SLS manufacturing process with the traditional process [16]. Based on an equipment energy consumption test, Xu et al. established a binder jetting AM energy consumption model that considered the part shape and process parameters [17]. Based on the convex function method, Paul et al. proposed an SLS energy consumption model based on part geometry, slice thickness, and printing direction process parameters, and proposed an optimization model to analyze the minimum energy consumption required in the AM process [18]. Ma et al. outlined an energy consumption model based on the SLS scanning speed, scanning gap, and layered thickness

85 process parameters. To improve energy efficiency, a multi-objective genetic algorithm was used to
86 optimize the process parameters [19].

87 Research on the environmental evaluation of AM processes is mainly carried out from two
88 perspectives. One is the comparison of the AM process with other processes from the perspective
89 of environmental benefits. Typical examples of this approach in the literature include Huang et al.,
90 who estimated the net changes in lifecycle primary energy and GHG emissions associated with
91 AM technologies for lightweight metallic aircraft components to shed light on the environmental
92 benefits of a shift from conventional manufacturing to AM processes in the U.S. aircraft industry
93 [20] and Kellens et al., who compared the environmental impact of different AM processes from
94 the existing lifecycle inventory data, considering energy consumption and material consumption in
95 the AM unit process [21].

96 The other aspect of environmental evaluation of AM is the sustainability assessment of AM
97 considering multiple factors. Bourhis et al. developed environmental impact prediction models to
98 analyze the environmental impact of electric energy and raw material consumption in the AM
99 process [22]. Li et al. established a cost model, energy consumption model, and model of product
100 surface roughness of AM parts, with the aim of evaluating the manufacturing cost and
101 environmental impact of different AM methods [23]. Kellens et al. evaluated the environmental
102 footprint of SLS, including the energy resource consumption and process emissions in its
103 manufacturing process, but energy consumption was the only quantitative indicator used for
104 environmental impact assessment [24]. Rejeski et al. described the potential environmental impact
105 of AM related to issues such as energy utilization, occupational health, waste, lifecycle analysis,
106 cross cutting, and policy issues, and introduced the latest technologies and research needs of AM

into this discussion [25]. Peng et al. analyzed the energy consumption and environmental impact of AM from a sustainability perspective [26].

As these studies indicate, many analysis methods and quantitation models have been proposed to address the energy consumption and environmental impact of AM. Nevertheless, these methods are usually focused on only one AM process, such as FDM, stereolithography (SLA), or SLS; no general modeling method for AM has yet been proposed. The existing established processing energy consumption models for different AM processes are based on energy measurement of different equipment. Hence, different AM parts have different energy consumption models, which leads to a difficult energy consumption modeling process and slow energy consumption quantitation process. Therefore, there is still a lack of a common model and quantitation method for the energy consumption of complex AM part processing by different kinds of AM technologies. Based on previous research on energy consumption modeling and estimation methods applicable to different AM processes, a feature-based energy consumption quantitation strategy for complex AM parts is proposed in this study. Based on this method, the energy consumption and environmental impact of AM processes can be predicted before the manufacturing process, providing a basis for process optimization. In addition, real-time prediction of AM energy consumption can be implemented by integrating this method into the AM 3D software model, which would provide a reference for structural optimization of AM parts.

The remainder of this paper is organized as follows. In Section 2, the feature-based energy consumption and efficiency indicators for AM manufacturing of complex parts are analyzed and the models are developed. Then, a case study is set up to study the energy characteristics of three different kinds of AM processes by manufacturing typical mechanical parts to verify the feasibility

and effectiveness of this method in Section 3. The result, including the deviation and limitations of the proposed method, are presented and discussed in Section 4, and efficiency improvement strategies for AM are addressed. Finally, the conclusion and plans for future work are presented in Section 5.

2 Feature-based energy consumption model for AM parts

The energy consumption of AM can be divided into two categories: primary energy consumption and secondary energy consumption. Primary energy consumption refers to the energy used to change the form and properties of materials in the AM process, which can also be considered as the essential energy consumption or direct energy consumption in the AM process. The other energy used is called secondary energy consumption, which refers to the energy needed by the auxiliary components of AM equipment, such as the energy consumption of the motor or energy used for heating the workbench, to realize and support the AM process. It can also be regarded as indirect energy consumption, and is a process-dependent energy component that is highly influenced by the capability of the equipment (consumer components), product design (geometry and dimensions), and settings and conditions (e.g., layer thickness and part orientation). The energy consumption of necessary environmental safety equipment, such as a ventilation system, is also included in secondary energy consumption. This section presents the proposed model for quantitation of the energy consumption of AM part manufacturing.

2.1 System boundary

The energy consumption analysis and modeling of AM parts begins with the definition of the boundaries of the AM process. Figure 1 shows the system boundary for the feature-based energy

consumption analysis. Three dimensions of environmental impact factors are considered for analyzing the manufacturing process of AM parts: energy consumption, material consumption, and time consumption dimensions.

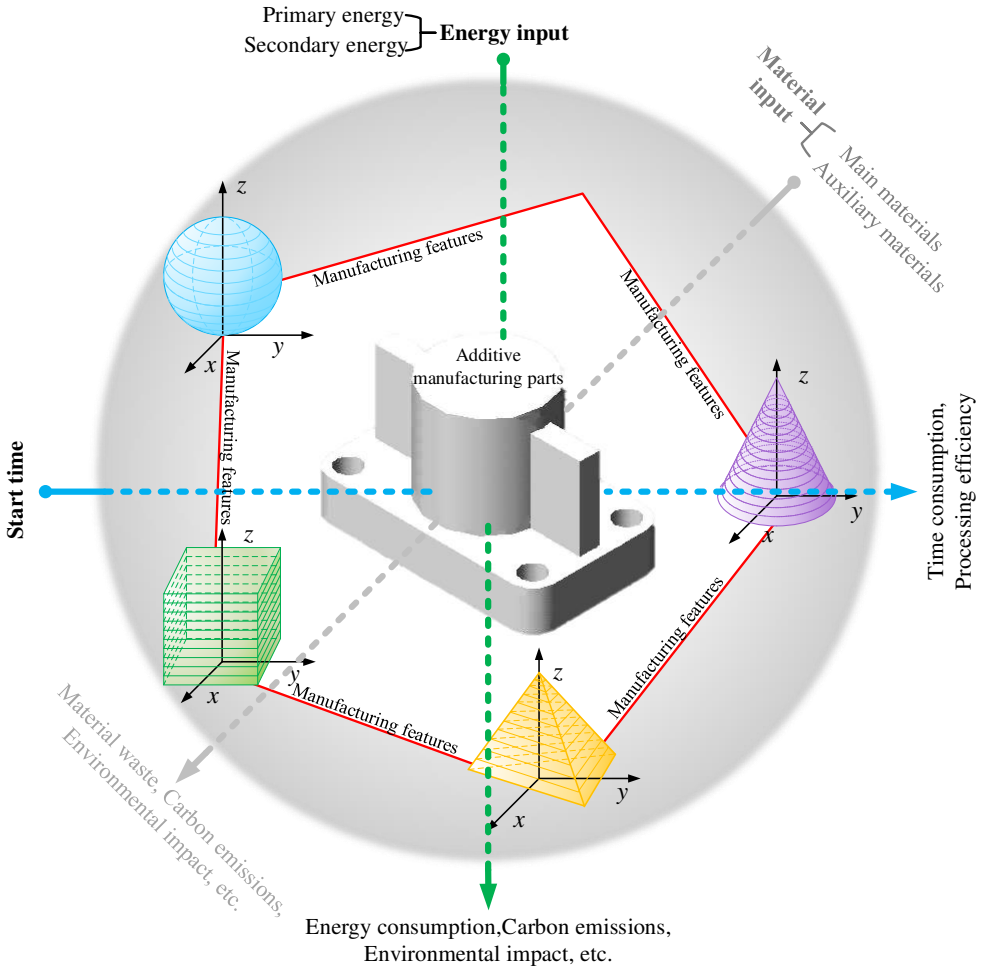

Figure 1 System boundary of feature-based energy consumption analysis of additive manufacturing (AM) parts

The energy consumption dimension includes the primary and secondary energy consumption of each manufacturing feature of the processed parts. The primary energy consumption used to change the material properties. The secondary energy consumption included in this model is only that directly related to part processing. The other energy consumed by the equipment has been analyzed and discussed in previous studies [27, 28], and is therefore not considered in this method.

160 The time consumption dimension includes the printing time and time needed for pre- and
161 post-processing. The printing time refers to the duration from the time of beginning workpiece
162 forming to the end of fabrication. The time consumed in the pre-processing and post-processing
163 stages of the parts is also considered in the entire time consumption evaluation.

164 The material consumption dimension is also an important factor in the environmental impact
165 of AM. It includes the direct material consumption for forming the part as well as the auxiliary
166 material consumed by printing supporting and adhesive structures. Moreover, the material
167 consumption is directly proportional to the energy consumption in the AM process. However, the
168 material consumption of AM parts was not the focus of this study; the proposed model directly
169 addresses only the energy consumption dimension.

170 **2.2 Method description**

171 AM parts are processed using layered stacking, and each manufacturing feature of the part
172 can be directly produced. The AM system can be divided into the following hierarchy, as shown in
173 Figure 2: the AM feature (AMF) layer, AM part layer, and AM equipment layer. All levels in the
174 system are related to each other through energy flow and material flow. An AMF is the basic
175 manufacturing unit of the system, and an AM part is composed of a series of AMFs. Therefore, the
176 energy consumption of each AM part can be obtained by analyzing the energy consumption of its
177 basic manufacturing features. Finally, the energy consumed by the material processing of the AM
178 equipment is also considered.

179 In the feature segmentation–based energy consumption analysis method, the AM parts are
180 divided into simple basic manufacturing features, AMF 1, AMF 2, … AMF *n*, on the basis of the

geometric features of the processed AM parts. Energy consumption models of each AMF are established, and the final energy consumption of the processed parts is determined by combining the AMFs. In this strategy, a part is decomposed into an aggregation of AMFs to collapse its geometric complexity for energy consumption calculation. Thus, the overall energy consumption of a complex AM part depends on the energy consumption analysis of each AMF. Consequently, the strategy is suitable for computer simulation.

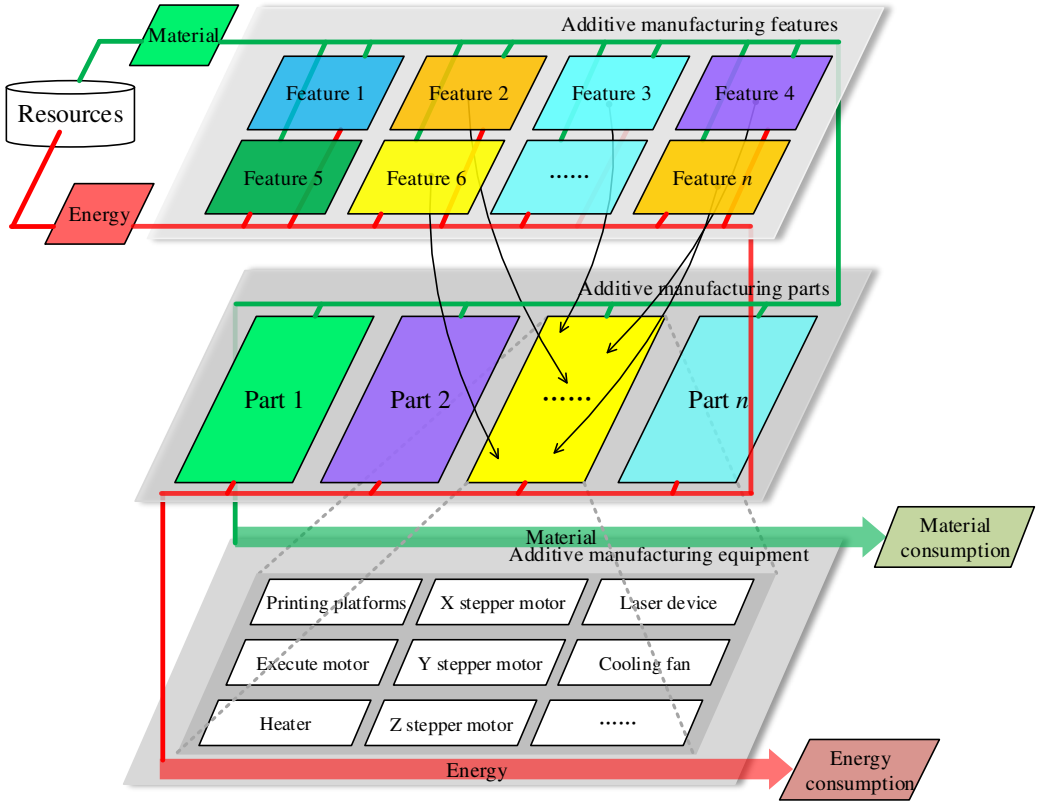

Figure 2 Schematic view and features of additive manufacturing (AM) system hierarchy

Using this analysis method, a complex profile AM part can be considered as a combination of its AMFs, regardless of the complexity of the final shape. Therefore, the total energy consumption for an AM part used to form the desired shape, E_{AMP}, is also the combination of the energy consumption of each AMF, and can be calculated by

$$E_{\mathrm{AMP}} = i_1 E_{\mathrm{AMF1}} + i_2 E_{\mathrm{AMF2}} + i_3 E_{\mathrm{AMF3}} + \mathrm{L} + i_n E_{\mathrm{AMF}n}, \quad (1)$$

where, i_1, i_2, …, i_n are the counts of each AMF and E_{AMF1}, E_{AMF2}, … , and $E_{\mathrm{AMF}n}$ are the energy consumption of each AMF.

2.3 Energy consumption model of AMFs

2.3.1 Assumptions and descriptions

Based on the geometric features of AM fabricated parts and basic manufacturing features obtained by feature segmentation, five typical manufacturing features are selected as AMFs for analyzing and modeling the energy consumption of various AM parts in this study. The five AMFs investigated are shown in Figure 3: hexahedron, sphere, cylinder, circular cone, and tetrahedron. The assumptions and explanations for the models are as follows:

- It is assumed that all AMFs are manufactured with uniform material distribution and no cracks or defects.
- The energy consumed by support manufacturing of AM parts could also be analyzed using the same feature-based energy consumption method. The influence of support on the energy consumption model of AMFs is not considered.
- Different manufacturing directions of AMFs affect the modeling method, but the final material consumption of the AMF is the same. The influence of manufacturing direction on the energy consumption model is ignored in the developed models. All the investigated energy consumptions of the AMFs are modeled using the manufacturing directions shown in Figure 3.
- Only five typical AMFs are taken as examples to model the energy consumption of AMFs, but this does not mean that there are only five basic AMFs. The energy consumption model

analysis methods of other features can be obtained by analogy to the proposed analysis methods.

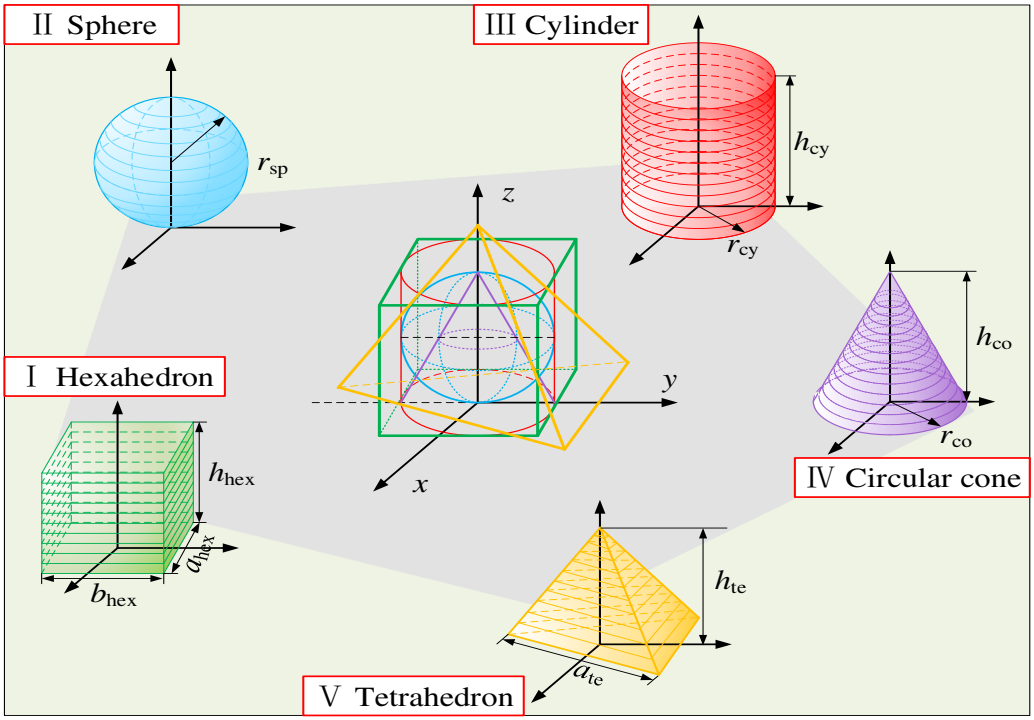

Figure 3 Typical additive manufacturing features (AMFs) and their related parameters

2.3.2 Energy consumption model of basic AMFs

The geometric parameters, layering mode, and manufacturing direction of each AMF modeled here are shown in Figure 3. According to the definition of the system boundary, the energy consumed directly by processing the AMF is considered during the energy consumption modeling process. Different processing paths and different AM methods will affect the energy consumption and models. The following four processing paths are considered, as shown in Figure 4: (a) square circle, (b) line, (c) grid, and (d) triangle. Three different AM methods are considered in energy consumption modeling of basic AMFs: FDM, SLA, and SLM.

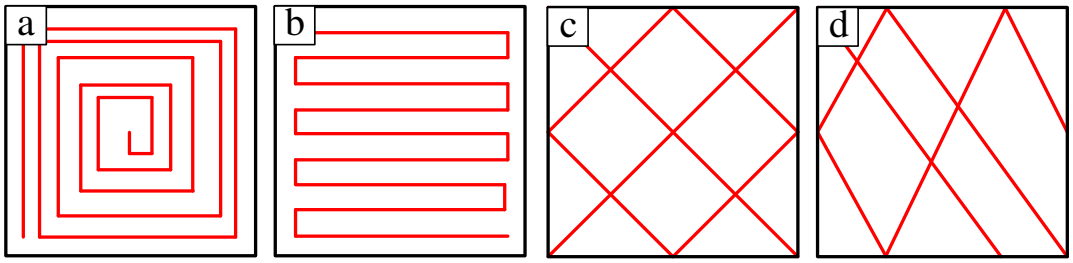

Figure 4 Different object in-fill patterns: (a) Square-circle; (b) Line; (c) Grid; (d) Triangle

The energy consumption of an AMF can be divided into two parts based on different AM equipment features. One is the main energy consumption, that is, the energy consumption used to change the material properties and form, such as the nozzle heating (in FDM), laser irradiation (in SLA), or laser melting (in SLM). This part of the energy consumed in this process is influenced by manufacturing parameters, and the processing parameters such as the layer thickness of the parts, scanning speed, and scanning gap. The other part is the auxiliary energy consumption, that is, the energy consumption of the actuator movement process, that is, the energy consumed by the scanning action of the nozzle or laser, which is influenced by the processing path, the movement of the plate, etc.. The energy consumption analysis for each basic AMF is as follows:

(1) Energy consumption model of the AMF hexahedron

Considering the geometric features of the hexahedron, and according to the slicing method shown in Figure 3, each layer has the same shape and size. The main energy consumption required for each layer of the AMF hexahedron, $E_{\text{hex}}^{\text{layer}}$, can be described as

$$E_{\text{hex}}^{\text{layer}} = a_{\text{hex}} b_{\text{hex}} l_{\text{lay}} P_{\text{mat}}, \tag{2}$$

where a_{hex} and b_{hex} are the bottom length and width of the AMF hexahedron, respectively; l_{lay} is the layer thickness; and P_{mat} is the energy consumption required to change the properties and state of the unit volume material.

The main energy consumption of the whole AMF hexahedron, $E_{\text{hex}}^{\text{main}}$, can be obtained by the following:

$$E_{\text{hex}}^{\text{main}} = \sum_{1}^{k} a_{\text{hex}} b_{\text{hex}} l_{\text{lay}} P_{\text{mat}} , \tag{3}$$

$$k = \frac{h_{\text{hex}}}{l_{\text{lay}}} , \tag{4}$$

where h_{hex} is the height of the AMF hexahedron and k is the number of layers of AMF hexahedrons.

The model of P_{mat} is different for different AM technologies. For FDM, P_{mat} can be obtained using Eqs. (5) and (6).

$$P_{\text{mat-h}} = 1000 c \rho \Delta t , \tag{5}$$

$$P_{\text{mat-m}} = q \rho , \tag{6}$$

where $P_{\text{mat-h}}$ is the energy consumption of material heating, $P_{\text{mat-m}}$ is the energy consumption of material melting, c is the specific heat capacity (kJ/kg•°C), ρ is the mass of material per unit volume(kg/m^3), Δt is the temperature difference (° C), and q is the enthalpy of fusion (J/kg).

For crystalline materials or eutectic mixtures, which have a fixed temperature in the melting stage (melting point), this part consists of two sub-components: heating energy and melting energy. For non-crystalline materials, the temperature continues to rise during the melting process; therefore, only Eq. (5) can be applied.

For SLA and SLM, in which a laser is used to change the material properties, $P_{\text{mat-l}}$ can be obtained by analyzing the laser energy consumption.

$$P_{\text{mat-l}} = \frac{\omega P_{\text{las}} \rho}{v_{\text{las}} A_s} , \tag{7}$$

where ω is the material absorptivity, P_{laser} is the rated power of the laser, v_{laser} is the laser scan

speed, and A_s is the area covered by the laser beam spot.

Because the laser beam passes through the lens, it is a Gaussian beam, so the laser energy in the spot follows a Gaussian distribution, and a parabolic shape is formed at the critical point of the sintering cross section. Thus, the area can be written as

$$A_s = \frac{2h_{\text{las}} l_{\text{lay}}}{3}, \tag{8}$$

where h_{las} is the gap distance.

Therefore, P_{mat} can be also given as

$$P_{\text{mat-l}} = \frac{3\omega P_{\text{las}} \rho}{2v_{\text{las}} h_{\text{las}} l_{\text{lay}}}. \tag{9}$$

The auxiliary energy consumption of the AMFs is affected by the processing time and movement speed of the actuator. Mathematically, the energy used for the auxiliary movement is defined as follows:

$$E_{\text{hex}}^{\text{aux}} = \sum_{1}^{k} \int_{t_1}^{t_2} P_{\text{aux}}(t) dt, \tag{10}$$

where P_{aux} is the power consumption of an auxiliary process, including the movement of the worktable, scraper, and powder feeding device; t_1 and t_2 are the starting and ending times of a single auxiliary action, respectively; and k is the number of auxiliary units.

Therefore, the total energy consumption of the AMF hexahedron, E_{hex}, is

$$E_{\text{hex}} = \sum_{1}^{\frac{h_{\text{hex}}}{t_{\text{lay}}}} a_{\text{hex}} b_{\text{hex}} l_{\text{lay}} P_{\text{mat}} + \sum_{1}^{k} \int_{t_1}^{t_2} P_{\text{aux}}(t) dt. \tag{11}$$

(2) Energy consumption model of the AMF sphere

The AMF sphere is sliced as shown in Figure 3, and circles with different radii are obtained for each sliced piece. The main energy consumption required for processing each layer of the

276 AMF sphere, E_{sp}^{layer}, can be given as follows:

$$E_{sp}^{layer} = \pi z\left(2r_{sp} - z\right) l_{lay} P_{mat}, \tag{12}$$

277 where r_{sp} is the radius of the AMF sphere.

278 The main energy consumption of the whole AMF sphere, E_{sp}^{main}, can be obtained using the

279 following equation:

$$E_{sp}^{main} = \int_0^{r_{sp}} \pi z\left(2r_{sp} - z\right) dz P_{mat}. \tag{13}$$

280 Therefore, the total energy consumption of AMF sphere, E_{hex}, is

$$E_{sp} = \int_0^{r_{sp}} \pi z\left(2r_{sp} - z\right) dz P_{mat} + \sum_1^k \int_{t_1}^{t_2} P_{aux}(t) dt. \tag{14}$$

281 (3) Energy consumption model of the AMF cylinder

282 Similar to the energy consumption analysis method of the AMF hexahedron, the AMF

283 cylinder is sliced as shown in Figure 3. The shape and size of each sliced piece are the same, and

284 the main energy consumed by processing each layer of the AMF cylinder, E_{cy}^{layer}, can be

285 expressed as

$$E_{cy}^{layer} = \pi r_{cy}^{\ 2} l_{lay} P_{mat}, \tag{15}$$

286 where r_{cy} is the radius of the AMF cylinder bottom.

287 The main energy consumption of the whole AMF cylinder, E_{cy}^{main}, can be given as

$$E_{cy}^{main} = \sum_1^{\frac{h_{cy}}{l_{lay}}} a\pi r_{cy}^{\ 2} l_{lay} P_{mat}, \tag{16}$$

288 where h_{cy} is the height of AMF cylinder.

289 Therefore, the total energy consumption of AMF cylinder, E_{hex}, is

$$E_{cy} = \sum_1^{\frac{h_{cy}}{l_{lay}}} a\pi r_{cy}^{\ 2} l_{lay} P_{mat} + \sum_1^k \int_{t_1}^{t_2} P_{aux}(t) dt. \tag{17}$$

290 (4) Energy consumption model of the AMF circular cone

291 The AMF circular cone is sliced as shown in Figure 3, and the shape of each layer is a circle
292 with a gradually reduced radius. The main energy consumption required for processing each layer
293 of the AMF circular cone, E_{sp}^{layer}, can be expressed as follows:

$$E_{co}^{layer} = \pi \frac{r_{co}^{\ 2}\left(h_{co}-z\right)^2}{h_{co}^{\ 2}} l_{lay} P_{mat}, \tag{18}$$

294 where r_{co} is the bottom radius of the AMF circular cone and h_{co} is the height of the AMF circular
295 cone.

296 Therefore, the total energy consumption required for processing the AMF circular cone, E_{co},
297 is

$$E_{co} = \pi \int_0^{h_{co}} \frac{r_{co}^{\ 2}\left(h_{co}-z\right)^2}{h_{co}^{\ 2}} dz P_{mat} + \sum_1^k \int_{t_1}^{t_2} P_{aux}\left(t\right) dt. \tag{19}$$

298 (5) Energy consumption model of the AMF tetrahedron

299 The AMF tetrahedron is sliced as shown in Figure 3. The shape of each layer is an equilateral
300 triangle with gradually reduced side length. The main energy consumption required for processing
301 each layer of the AMF tetrahedron, E_{te}^{layer}, can be expressed as follows:

$$E_{te}^{layer} = \frac{\sqrt{3}}{4} \frac{a_{te}^{\ 2}\left(h_{te}-z\right)^2}{h_{te}^{\ 2}} l_{lay} P_{mat}. \tag{20}$$

302 where a_{te} is the length of the AMF tetrahedron bottom and h_{te} is the height of the AMF
303 tetrahedron.

304 Therefore, the total energy consumption required for processing AMF hexahedron, E_{te}, is

$$E_{te} = \frac{\sqrt{3}}{4} \int_0^{h_{te}} \frac{a_{te}^{\ 2}\left(h_{te}-z\right)^2}{h_{te}^{\ 2}} dz P_{mat} + \sum_1^k \int_{t_1}^{t_2} P_{aux}\left(t\right) dt. \tag{21}$$

2.3.3 General model of energy consumption for AMFs

Based on the energy consumption analysis and modeling method for the five basic AMFs described in Section 2.3.2, the AMF obtained by feature segmentation is manufactured in the direction of the least support method. A series of similar figures are obtained when the AMFs are sliced along the direction parallel to the workbench. The shape feature equation of each layer can be expressed as $f(x, y, z)$, and the general model of the main energy consumption for processing each layer of the AMF, $E_{\text{gene}}^{\text{layer}}$, can be described as

$$E_{\text{gene}}^{\text{layer}} = \int_{y_1}^{y_2} \int_{x_1}^{x_2} f(x, y, \text{z}) dx dy l_{\text{lay}} P_{\text{mat}}, \tag{22}$$

where x_1 and x_2 are the limits of each layer shape on the x-axis, and y_1 and y_2 are the limits of each layer shape on the y-axis.

Taking the auxiliary energy consumption of the AMFs into account, the general model of energy consumption for AMFs, E_{gene}, can be given as follows:

$$E_{\text{gene}} = \int_0^h \int_{y_1}^{y_2} \int_{x_1}^{x_2} f(x, y, \text{z}) dx dy dz P_{\text{mat}} + \sum_1^k \int_{\Delta t} P_{\text{aux}}(t) dt. \tag{23}$$

where h is the height of AMF, and Δt is the interlayer auxiliary action time.

The general model of AMFs can be used to analyze and quantify the energy consumption of all kinds of multi-feature AM parts. The basic AMFs can be obtained by the feature segmentation method. In the process of feature segmentation, the divided basic features should be as simple as possible to improve the efficiency and reliability of the energy consumption quantitation results.

2.4 Efficiency indicators of AM

Based on the proposed energy consumption quantitation strategy of AM and energy efficiency analysis method for machine tools, the energy and production efficiency of AM

machines are analyzed for the following work of energy-saving optimization and production efficiency improvement of the workshop. The indicators of AM energy efficiency and time efficiency are developed in this section.

2.4.1 Energy efficiency of the AM machine

Based on the energy consumption models developed in Section 2.3, and the energy consumption stages of the AM process, including the pre-processing preparation stage, parts shaping stage, post-processing stage, and machine waiting, the effective energy consumption of the AM process is mainly used for the parts shaping process. Thus, the energy efficiency of different AM machines can be expressed as

$$\eta_{\mathrm{e}} = \frac{E_{\mathrm{AMP}}}{E_{\mathrm{T}}}, \tag{24}$$

in which

$$E_{\mathrm{T}} = \sum_{n} E_i \left(i \text{ is different stage in AM process} \right), \tag{25}$$

where η_{E} is the energy efficiency of the AM machine, E_{T} is the total energy consumption of the whole AM process, and E_i is the energy consumption of different stages in the AM process, which are pre-stage, forming stage, post-processing stage, and idle stage.

2.4.2 Time efficiency for the AM process

Time consumption of AM has a significant impact on inventory cost, production planning, and scheduling in an AM factory. The time efficiency of AM can be defined as the ratio of the effective forming time of a part to the total length of the AM process, which can be expressed as

$$\eta_{\mathrm{t}} = \frac{t_{\mathrm{AMP}}}{T_{\mathrm{T}}}, \tag{26}$$

$$T_{\mathrm{T}}=\sum_{n} t_i \left(i \text{ is different stage in AM process}\right), \tag{27}$$

where η_{P} is the time efficiency of the AM machine; t_{AMP} is the forming processing time of the parts; T_{T} is the total time consumption of the whole AM process; T_i is the energy consumption of different stages in the AM process, which are the pre-stage, forming stage, post-processing stage, and idle stage.

3 Case study

To verify the accuracy and feasibility of the proposed feature-based energy consumption quantitation strategy, a case study was conducted. The energy consumption models of typical AMFs were applied to evaluate the energy consumption of the AM parts shown in Figure 5. The shape and size parameters of the selected parts are listed in Table 1. In order to verify the generality of the developed models, the predicted energy consumption was compared with experimental results obtained using different AM methods. Three kinds of AM technologies were used to fabricate the part: FDM, SLA, and SLM.

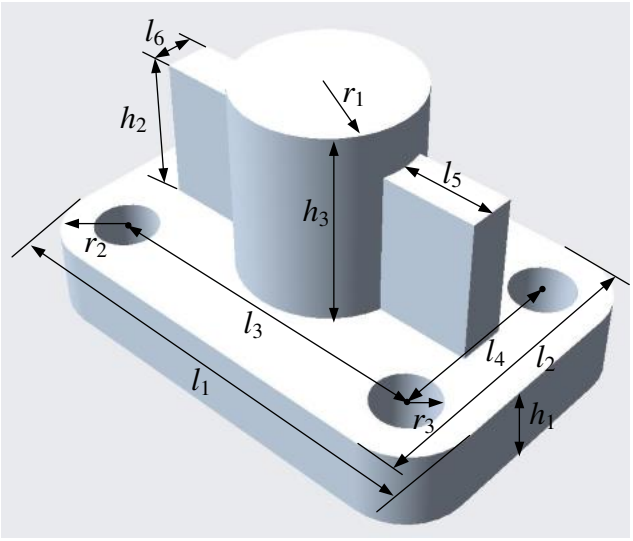

Figure 5 Computer-aided design (CAD) model of the processed additive manufacturing (AM) parts

355 Table 1 Shape and size parameters of the processed additive manufacturing (AM) parts

Parameter	Value (mm)
l_1	40
l_2	28
l_3	28
l_4	16
l_5	7
l_6	4
r_1	8
r_2	6
r_3	3
h_1	6
h_2	12
h_3	16

356 The process parameters of the three types of AM processing method were determined to
357 ensure the forming quality of the processed parts. The main parameters for FDM, SLA, and SLM
358 are shown in Table 2.

359 Table 2 Parameter for different additive manufacturing g(AM) technology processes

Processing mode	Material	Layer thickness l_{lay} (mm)	Nozzle heating temperature t (°C)	Laser power P_{las} (W)	Scanning speed v (mm/s)	Scanning path

FDM	PLA	0.1	210	-	100	(c) Grid
	SOMOS					
SLA	Imagine 8000	0.1	-	0.8	232	(c) Grid
	resin					
SLM	316L powder	0.02	-	500	7000	(c) Grid

3.1 Feature division of the manufactured AM part

According to the shape features of the AM parts and the proposed feature segmentation method, the parts are divided into seven AMFs, as shown in Figure 6. The obtained AMF1 is a cylindrical feature, AMF6 is a removed cylinder feature, and AMF3, AMF4, and AMF5 are hexahedral features. The manufacturing features of AMF2 are approximated by hexahedral manufacturing features. AMF7 is a quarter cylinder manufacturing feature, and four AMF7s form a whole cylinder.

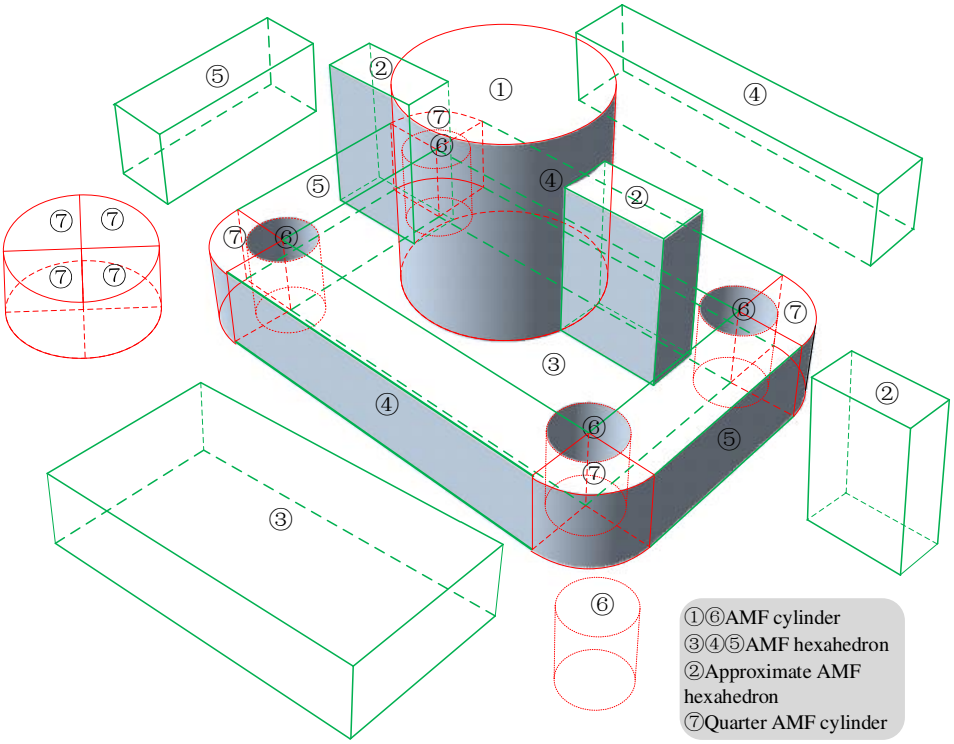

Figure 6 Manufacturing feature segmentation of processed additive manufacturing (AM) parts

3.2 Theoretical energy consumption model of the investigated AM part

Based on the energy consumption analysis and modeling method of typical AMFs, and the shape and size parameters of the processed AM parts in Table 1, the total energy consumption of the investigated AM part, E_{AMP}, is obtained based on each AMF in Figure 6, which can be expressed as

$$E_{\mathrm{AMP}} = E_{\mathrm{AMF1}} + 2E_{\mathrm{AMF2}} + E_{\mathrm{AMF3}} + 2E_{\mathrm{AMF4}} + 2E_{\mathrm{AMF5}} - 4E_{\mathrm{AMF6}} + 4E_{\mathrm{AMF7}} + E_{\mathrm{aux}}, \tag{28}$$

where E_{AMF1}, E_{AMF2}, E_{AMF3}, E_{AMF4}, E_{AMF5}, E_{AMF6}, and E_{AMF7} are the energy consumptions of AMF1, AMF2, AMF3, AMF4, AMF5, AMF6, and AMF7, respectively, and E_{aux} is the auxiliary energy consumption. The auxiliary energy consumption of all segmented manufacturing features is comprehensively considered to simplify the calculation.

Based on the energy consumption model established for the AMF cylinder, considering the shape and size parameters of the investigated AM part, the energy consumption of AMF1, AMF6, and AMF7 can be obtained by Eqs. (25)–(27).

$$E_{\mathrm{AMF1}} = \sum_{1}^{\frac{h_3}{l_{\mathrm{lay}}}} \pi r_1^2 l_{\mathrm{lay}} P_{\mathrm{mat}} , \tag{29}$$

$$E_{\mathrm{AMF6}} = \sum_{1}^{\frac{h_1}{l_{\mathrm{lay}}}} \pi r_3^2 l_{\mathrm{lay}} P_{\mathrm{mat}} , \tag{30}$$

$$E_{\mathrm{AMF7}} = \frac{1}{4} \sum_{1}^{\frac{h_1}{l_{\mathrm{lay}}}} \pi r_2^2 l_{\mathrm{lay}} P_{\mathrm{mat}} . \tag{31}$$

Based on the energy consumption model established for the AMF hexahedron, the energy consumption of AMF2, AMF3, AMF4, and AMF5 can be obtained by Eqs. (32)–(35).

$$E_{\mathrm{AMF2}} = \sum_{1}^{\frac{h_2}{l_{\mathrm{lay}}}} l_4 l_5 l_{\mathrm{lay}} P_{\mathrm{mat}} , \tag{32}$$

$$E_{\mathrm{AMF3}} = \sum_{1}^{\frac{h_1}{l_{\mathrm{lay}}}} l_2 l_3 l_{\mathrm{lay}} P_{\mathrm{mat}} , \tag{33}$$

$$E_{\mathrm{AMF4}} = \sum_{1}^{\frac{h_1}{l_{\mathrm{lay}}}} l_2 r_2 l_{\mathrm{lay}} P_{\mathrm{mat}} , \tag{34}$$

$$E_{\mathrm{AMF5}} = \sum_{1}^{\frac{h_1}{l_{\mathrm{lay}}}} r_2 l_3 l_{\mathrm{lay}} P_{\mathrm{mat}} . \tag{35}$$

The auxiliary manufacturing process is different in different AM machines with different processing modes. The auxiliary energy consumption for FDM, SLA, and SLM AM machines are considered separately.

For the FDM process, the auxiliary energy consumption is consumed by the process of plate movement, maintaining the plate temperature and nozzle movement, and the energy consumption of the auxiliary system of the LCD screen and LEDs, which can be described as follows:

$$E_{\text{aux}}^{\text{FDM}} = E_{\text{pla}} + E_{\text{hea}} + E_{\text{noz}} + E_{\text{sys}} . \tag{36}$$

389 Considering the parameters and processing process of the AM part, it can also be expressed

390 as

$$E_{\text{aux}}^{\text{FDM}} = \sum_{1}^{(h_1+h_3)/l_{\text{lay}}} \int_{\Delta t_1} P_{\text{mot1}}(t)dt + \int_{\Delta t_2} P_{\text{hea}}(t)dt + \int_{\Delta t_3} P_{\text{mot2}}(t)dt + \int_{T} P_{\text{sys}}(t)dt , \tag{37}$$

391 where P_{mot1} is the driven motor power of the plate, P_{hea} is the power for maintaining the plate

392 temperature, P_{mot2} is the driven motor power of the nozzle, P_{sys} is the power of the machine

393 auxiliary system, and T is the part processing time.

394 For the SLA process, the auxiliary energy consumption for the parts mainly includes the

395 energy consumption of plate moving, scraper movement, and auxiliary system, which can be

396 calculated by the following equation:

$$E_{\text{aux}}^{\text{SLA}} = \sum_{1}^{(h_1+h_3)/l_{\text{lay}}} \int_{\Delta t_4} P_{\text{mot1}}(t)dt + \int_{\Delta t_5} P_{\text{mot3}}(t)dt + \int_{T} P_{\text{sys}}(t)dt , \tag{38}$$

397 where P_{mot3} is the driven motor power of the scraper.

398 For the SLM process, the auxiliary energy consumption includes the energy consumption of

399 plate moving, scraper movement, power feeding movement, protective gas filling, cooling system,

400 and auxiliary system, which can be calculated by the following equation:

$$E_{\text{aux}}^{\text{SLM}} = \sum_{1}^{(h_1+h_3)/l_{\text{lay}}} \int_{\Delta t_6} P_{\text{mot1}}(t)dt + \int_{\Delta t_7} P_{\text{mot3}}(t)dt + \int_{\Delta t_8} P_{\text{mot4}}(t)dt + \int_{\Delta t_9} P_{\text{cool}}(t)dt + \int_{T} P_{\text{sys}}(t)dt , \tag{39}$$

401 where P_{mot4} is the driven motor power of the powder-feeding device, P_{cool} is the power of the

402 cooling device, and Δt_i (i = 1–9) is the action time of the corresponding moving parts.

403 **3.3 Energy consumption measurements of different printing modes**

404 An AWS2103S Plus power measurement three-phase power analyzer was used to perform the

405 energy measurement of the three kinds of AM machines, which are JGAURORA-A8S (FDM
406 machine), UNIONTECH-RS3000 (SLA machine), and BLT-S210(SLM machine). This power
407 meter has an accuracy of 0.5% ± 0.15% of range error and ± 0.15% of sensor error, with a 0.01s
408 sampling interval. The power consumed for each set of samples can be distinguished through
409 observations during the part forming processes and using the power-consumption-versus-time
410 profiles. The consumed electrical energy of each set of samples was calculated by the product of
411 the power and the time taken for the corresponding set of samples. Because of the two-phase
412 power input in the three AM machines, a single power measurement mode of the power meter is
413 selected to conduct the power measurement. The detailed output power date processing of the
414 power meter is as follows:

415 In single-phase power measurement, the load voltage and current are simultaneously
416 measured. A voltage unit and a current unit are used to measure the voltage and current in real
417 time. The apparent power can be obtained by multiplying the measured voltages U and I, and then
418 multiplying by the power factor, as shown in Eq. (40).

$$P_t = UI\cos\varphi, \tag{40}$$

419 where P_t is the measured apparent power and cos φ is the power factor.

420 The voltage and current signals are digitized to obtain the voltage sequence $U[n]$ and current
421 sequence $I[n]$, and then the instantaneous power sequence $P[n]$ is obtained. The average value of
422 the instantaneous power sequence $P[n]$ is the true power value, which is also known as the true
423 active power P_m.

$$P[n] = U[n] * I[n] \tag{41}$$

$$P_{\mathrm{m}} = \sum_{i=0}^{n-1} P[n] / n \,, \tag{42}$$

where $U[n]$ and $I[n]$ are the measured voltage and current sample sequences in the power meter, respectively.

In the experiment processes, three kinds of AM machines were used to process the parts shown in Figure 5 under the process parameters listed in Table 2. The voltage probe was plugged into the two-phase power inlet of the AM machines to measure the voltage value in real time. The current clamp was plugged directly into the stripped supply power cable in the power socket exit. Hence, the energy loss due to the electric transformer was taken into account for the electrical energy study. The measured instant power data were saved and processed to the power meter software on a computer. Figure 7 shows the electrical assembly diagram.

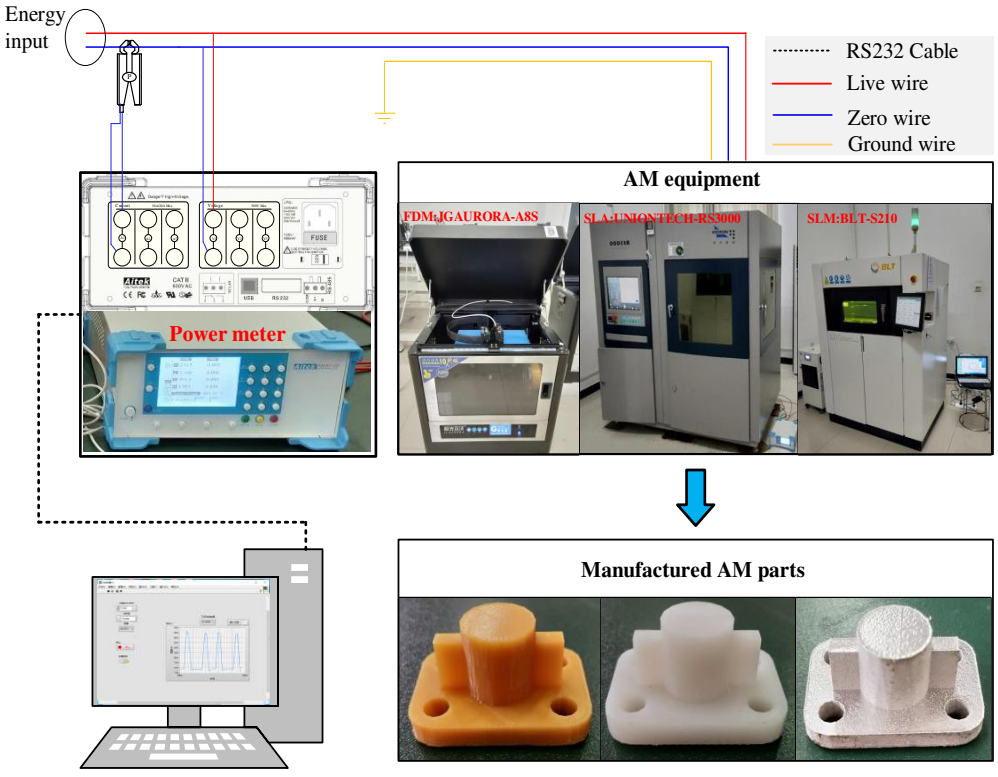

Figure 7 Schematic of the experimental testing system

435 # 4 Results and discussion

436 ## 4.1 Experimental verification of proposed energy quantitation method

437 The consumed energy of each process in forming the same AM part was measured according
438 to the energy consumption measurement method for each AM machine. The obtained power
439 consumption vs. time curves for the FDM, SLA, and SLM machines are shown in Figure 8, Figure
440 9 and Figure 10, respectively.

441 For the FDM forming process of a given part, the power variation curve of the machine after
442 the slice model of the part was imported into the machine system is shown in Figure 8. The power
443 measurement started while the machine was in standby mode. In this mode, the machine is not
444 printing; however, a small amount of electrical power is consumed because of the LCD screen and
445 LEDs. Then, the operator pressed the cycle start button and the warm-up stage began. The first
446 level of power corresponds to the rising temperature of the heat bed plate. The second level of
447 power corresponds to the nozzle warm-up. During this second level, the heat bed plate continues
448 to warm up until the temperature set point is reached. After all the components have finished their
449 warm-up stage, the forming stage starts. The forming process of a part includes bottom supporting
450 structure processing, which is mainly used for the connection of parts and plate, and the structure
451 processing of the part.

452 For the SLA forming process of a given part, after the processing model is imported into the
453 AM machine, the processing begins with work platform preparation, as shown in Figure 9. In the
454 initialization stage, the workbench moves to the highest level of resin to prepare for the part
455 forming process. The energy consumption in this stage depends on the power of the workbench

456 motor and other auxiliary structures of the machine. After that, the part is processed in the next
457 stage, which includes the forming process of the supporting structure and part structure. Although
458 there is no cantilever or hollow structure in the designed part, a 3 mm mesh solid support is added
459 at the bottom of the designed model for easy removal of the part from the workbench and to
460 ensure the dimensional accuracy of the part. The electrical energy consumed in the part processing
461 stage is determined by the part volume, build direction, support design, number of layers, and
462 machine auxiliary energy consumption. After the part has been finished, the workbench moves up
463 slowly from the resin to the highest position, and then the machine waits.

464 For the SLM forming process of a given part, after the processing model is imported into the
465 AM machine, the SLM process begins in a pre-processing stage, as shown in Figure 10. The
466 pre-processing stage includes pumping out air and filling with inert gas, and an intermittent
467 cooling cycle of the whole machine. After the pre-processing stage, the processing stage begins
468 with the formation of the bottom 3 mm mesh solid support and the structure of the part. The
469 energy consumed in this stage depends on the powder layering, laser scanning parts and supports,
470 and air pumping and aerating and cooling cycles. The post-processing stage starts after the entire
471 part is built. The machine is in standby mode in this stage. The electrical energy consumed in the
472 pre- and post-processing stages is determined by the SLM system and is relatively stable for each
473 SLM process.

474 The different AM machines have different processing stages during manufacturing the same
475 part. Based on the obtained power consumption curves for the three AM processing modes (Figure
476 8, Figure 9 and Figure 10), the corresponding measured energy consumption $E_{\mathrm{AMP}}^{\mathrm{ex}\text{-}j}$ (j = FDM,
477 SLA, or SLM), which is the energy consumed in the parts forming stage, and the total energy

consumption of the three different AM processes $E_{\mathrm{T}}^{\mathrm{ex}\text{-}j}$, and the corresponding time consumption are shown in Table 3. The efficiency indicators, including the energy efficiency of the AM machine η_{E}^{j}, and the time efficiency for the AM process η_{t}^{j} can be obtained based on Eqs. (24)–(27).

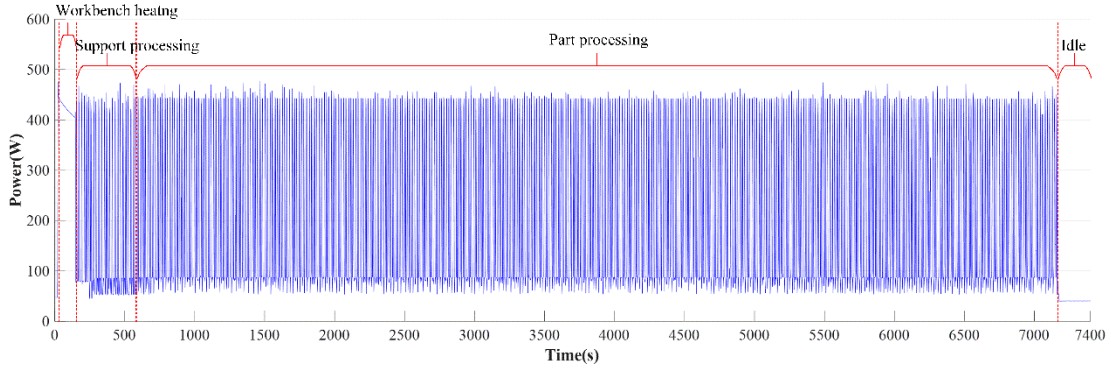

Figure 8 Power consumption vs time for an entire FDM process

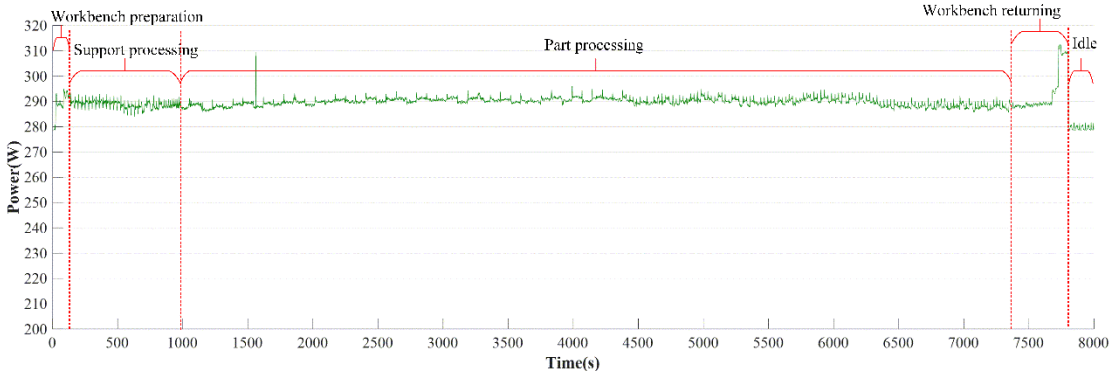

Figure 9 Power consumption vs time for an entire SLA process

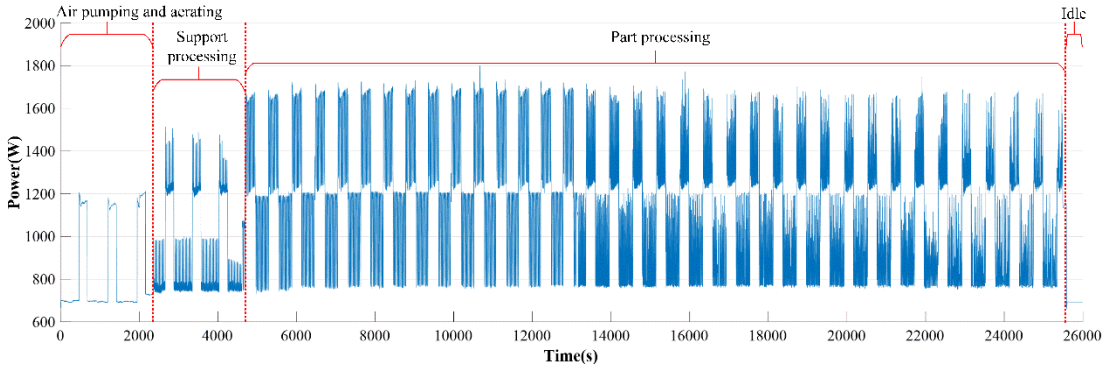

Figure 10 Power consumption vs time for an entire SLM process

On the basis of the developed energy consumption model of AM parts based on the feature segmentation method, after all the parameters were substituted into Eqs.(28)–(39), the theoretical forming energy, $E_{\mathrm{AMP}}^{\mathrm{th}\text{-}j}$, was obtained by the models for different processing modes, as shown in Table 3. The deviation rate ΔE_j between the part processing energy obtained by the models and experiments can be calculated using Eq.(43). A comparison of the results is shown in Figure 11.

$$\Delta E_j = \left| \frac{\left(E_{\mathrm{AMP}}^{\mathrm{th}\text{-}j} - E_{\mathrm{AMP}}^{\mathrm{ex}\text{-}j} \right)}{E_{\mathrm{AMP}}^{\mathrm{th}\text{-}j}} \right| \times 100\% \ , \ \left(j \text{ is FDM,SLA or SLM} \right). \tag{43}$$

Table 3 Energy consumption and efficiency indicators comparison for different AM mode

Processing mode	$E_{\mathrm{AMP}}^{\mathrm{ex}\text{-}j}$ (kJ)	$E_{\mathrm{AMP}}^{\mathrm{th}\text{-}j}$ (kJ)	$E_{\mathrm{T}}^{\mathrm{ex}\text{-}j}$ (kJ)	t_{AMP}^{j} (s)	T_{T}^{j} (s)	ΔE_j	η_{E}^{j}	η_{t}^{j}
FDM	1222.908	1201.899	1361.763	6582.498	8599	1.75%	89.80%	76.55%
SLA	1840.781	1728.424	2316.870	6349.441	8598	6.50%	79.45%	73.85%
SLM	23669.116	17948.360	28144.673	20813.919	32855.881	9.02%	84.10%	63.35%

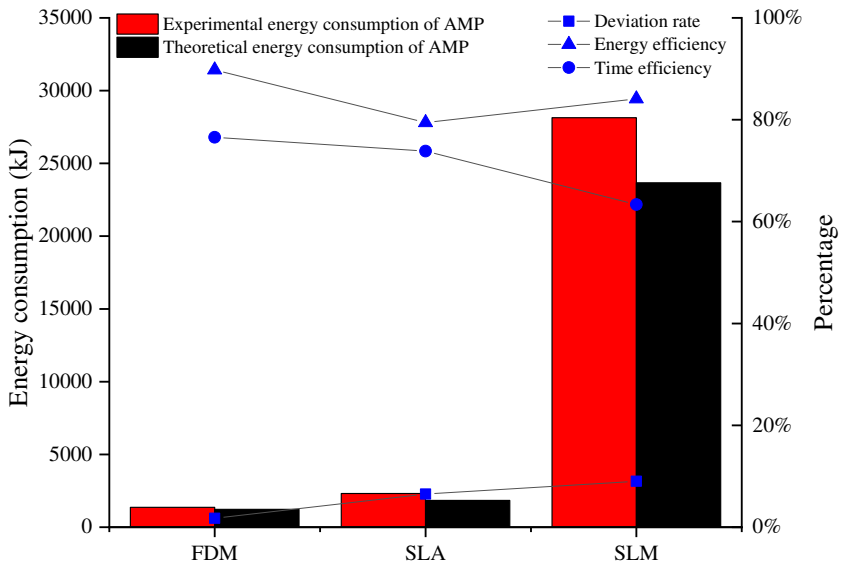

Figure 11 Energy consumption and efficiency indicators comparison under different AM technologies

The comparative results (Figure 11) show good coincidence for different AM technologies between the part processing energy consumption obtained from the proposed models and the experiments. The deviation is within the range of 10%, which means that the model catches the forming principle of the AM process. The energy consumption of the same part processed by different AM methods is quite different. From the efficiency analysis, it can be seen that the energy efficiency of the three different AM machines is approximately 80%, among which the FDM machine has the highest energy efficiency in the parts processing process. However, the time efficiency of the machines is relatively low: 76.55%, 73.85%, and 63.35% for FDM, SLA, and SLM, respectively. The time efficiency of the SLM process was the lowest.

4.2 Discussion

4.2.1 Deviation analysis

The comparison of the theoretical and experimental results verified that the developed models are adequately accurate for the energy consumption prediction of AM parts manufacturing. However, the process energy in all experimental runs was overestimated, which is a systematic deviation related to the error of the auxiliary system energy consumption between the calculated theoretical energy consumption and measured experimental energy consumption. The main reason is that the power of each energy consumption unit in the auxiliary system fluctuates in the processing process, and there is a gap between the actual power and its rated power value. The error between the model and actual energy consumption increases gradually with the number of energy consumption units in the AM system. The gap between the model and experience can be further reduced by considering the power fluctuation of the auxiliary energy consumption units.

517 In addition, in the development of the theoretical models, some basic assumptions are
518 essential to simplify the complexity of the calculation, which may cause deviation from the true
519 energy consumption quantity. In these models, some AMFs with irregular shapes and structures
520 obtained after segmentation are simplified. For example, the manufacturing features of AMF2 are
521 simplified into hexahedral manufacturing features in model development, but it is unchanged in
522 the experimental process, which also causes a systematic deviation. In order to achieve more
523 accurate models, some correction coefficients could be used to decrease these deviations.

524 Finally, in the experimental energy consumption measurement, the electrical energy
525 consumption of the input terminal is measured directly by a power meter. Hence, the energy loss
526 due to the electric transformer was taken into account for the experimental electrical energy study.
527 In addition, owing to machine aging, reduced accuracy of the machine control system, the
528 scanning speed, and the power of the laser could also lead to deviation.

529 *4.2.2 Power consumption feature analysis*

530 From the forming stage of the FDM process, many disruptions can be observed during this
531 last stage. These oscillations are not generated by the stepper motors. Indeed, values of current and
532 voltage are the same throughout the forming stage because of the nature of the motors.
533 Oscillations are generated by the maintenance of the heat-bed plate. Figure 12(a) shows a
534 zoomed-in section of the forming stage. This physical phenomenon lasts only 1–2 s and is
535 repeated throughout the forming stage.

536 From the power consumption vs. time curve of the whole SLA process, it can be seen that the
537 forming power of the machine is basically stable within a certain power range, and there is no

large power fluctuation. A zoomed-in section of the SLA forming stage is shown in Figure 12(b). The reason is that the laser power of the SLA machine is small, and a plate warm-up stage is not needed. The energy consumed in the whole forming process is mainly determined by the auxiliary system, stepper motor of each axis, and laser galvanometer motor. Hence, the power fluctuation is not large in the SLA process.

For the power consumption vs. time curve of the SLM process, the power consumption in the processing stage shows periodic fluctuations of different frequencies with large amplitude and small amplitude, as shown in Figure 12(c). Periodic power fluctuations with large amplitudes and low frequencies are caused by the periodic cooling water circulation of the machine system. The amplitude of the process is stable, and the cycle period is stable. For small amplitude and high-frequency power fluctuation, the main reason is the power fluctuation caused by the energy consumption of laser scanning for each layer of parts, and the cycle of the power fluctuation is related to the laser scanning time.

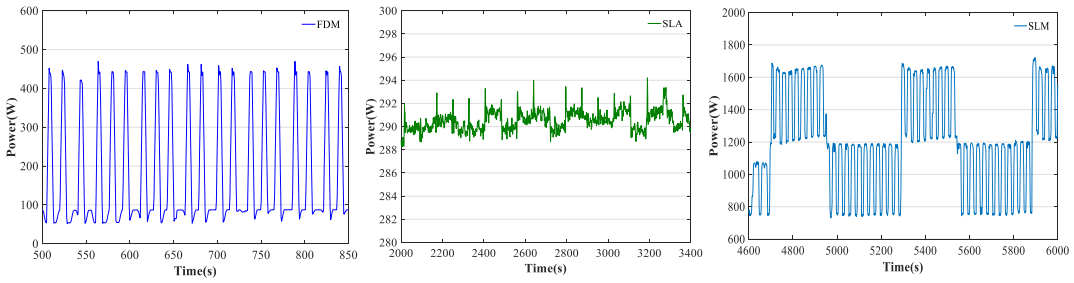

(a) (b) (c)

Figure 12 Zoomed-in section of power during the forming stage: (a) FDM process, (b) SLA process, (c) SLM process

555 *4.2.3 Efficiency improvement methods*

556 Based on the above comparison results of energy consumption and efficiency indicators, it
557 can be found that although the energy efficiency of AM machines is higher, there is still room for
558 improvement. Based on power consumption–time curves for FDM, SLA, and SLM machines and
559 power consumption feature analysis for different AM processes, the following measures can be
560 taken to improve the energy efficiency and production and processing time energy efficiency of
561 AM:

562 (1) Reduce auxiliary energy consumption of equipment. The reason for the relatively low
563 energy efficiency of the SLA and SLM machines is that their auxiliary energy consumption is
564 higher. Therefore, for different AM machines, there are different means to reduce the auxiliary
565 energy consumption.

566 For the FDM machine, select a reasonable heating plate and nozzle heating temperature, and
567 optimize the machine cooling system to reduce the energy consumption of the heating and cooling
568 processes, and reduce the waiting time of the machine.

569 For the SLA machine, the auxiliary energy consumption caused by too many auxiliary energy
570 consumption units can be improved by optimizing the equipment structure and simplifying the
571 auxiliary unit.

572 For SLM machines, the energy efficiency of the auxiliary equipment of the machine should
573 be optimized, such as improving the energy efficiency of the equipment cooling system and
574 reducing the waiting time of the machine.

575 (2) Reasonable placement design and production batches of the parts. According to the
576 platform size of different AM machines, make full use of the platform to form multiple parts at a

time. Selecting parts with similar structures and heights to be processed in a batch can not only improve the energy efficiency of the equipment, but also increase the effective processing time and production efficiency of the process.

5 Conclusions

To solve the problem of energy consumption quantitation of complex AM parts and improve the energy and production efficiency of AM, this paper proposes a feature-based energy consumption quantitation method and develops a comprehensive model of energy consumption for complex AM parts. In this strategy, a feature segmentation method is proposed to divide complex AM parts into typical AMFs. The energy models of each AMF were established to predict the energy consumption of the whole part. The energy consumption characteristics of a typical mechanical part manufactured by three different kinds of AM processes, namely FDM, SLA, and SLM, were studied by the proposed feature-based energy consumption quantitation method and compared with experimental energy consumption measurements. The results show that the proposed method can effectively and quickly predict the energy consumption of AM parts. To clarify the equipment energy efficiency and production efficiency of the three different technologies, the corresponding energy efficiency indicators were established, and the energy efficiency and time efficiency characteristics of the three AM processes were analyzed and compared. Corresponding suggestions and methods to improve the energy efficiency and production efficiency of AM were proposed. This model allows users to predict the energy consumption and environmental impact of their AM parts during the product design stage.

Future work will be devoted to integrating the method into the 3D software post-processing

598 analysis of different AM machines, so as to realize the energy consumption prediction of different
599 AM machines before part processing, which can provide a reference and basis for the research of
600 AM parameter optimization and energy-saving methods for AM machines.

601 ## Availability of data and materials

602 All data generated or analysed during this study are included in this published article.

603 ## Competing interests

604 The authors have declared that no competing interests exist.

605 ## Funding

606 This work was supported by the National Natural Science Foundation of China (NO.
607 51775162), Natural Science Foundation of Anhui Province (2008085QE265, 2008085QE232,
608 2008085ME150), Suzhou Engineering Research Center for Collaborative Innovation of
609 Mechanical Equipment (SZ2017ZX07), Anhui Major Science and Technology Project
610 (18030901023), and Opening Project of Suzhou University Research Platform (2019kyf21,
611 2019ykf26, 2019ykf27).

612 ## Authors' contributions

613 Mengdi Gao contributed to the conception of the study, and wrote the manuscript;
614 Lei Li, Qingyang Wang and Zhilin Ma performed the experiments;
615 Xinyu Li contributed significantly to analysis and manuscript preparation;
616 Conghu Liu performed the data analyses;

Zhieng Liu helped perform the analysis with constructive discussions.

Reference

[1] China Business Information Network. China Business Industry Research Institute released a research report on 3D printing industry market Prospect and investment in 2019. [cited 2019]Available from: http://www.askci.com/news/chanye/20190422/0929591145108_2.shtml.

[2] 《Wohlers Report》.[cited]Available from: http://www.wohlersassociates.com/.

[3] Paolini A, Kollmannsberger S, Rank E. Additive manufacturing in construction: A review on processes, applications, and digital planning methods [J]. Additive Manufacturing 2019, **30:** 100894.

[4] Tuan, D., Ngo, Alireza, Kashani, Gabriele, Imbalzano, Kate, T.Q. Additive manufacturing (3D printing): A review of materials, methods, applications and challenges [J]. Composites Part B-engineering, 2018: 172-196..

[5] Gao W, Zhang Y, Ramanujan D, Ramani K, Chen Y, Williams CB, Wang CC, Shin YC, Zhang S, Zavattieri PD. The status, challenges, and future of additive manufacturing in engineering [J]. Computer-Aided Design, 2015, **69:** 65-89.

[6] Yang, X., More efforts are needed to promote new energy [Online]. [cited]Available from:: energy.people.com.cn/n1/2019/0307/c71661-30961766.html (accessed on 21 Jan. 2020).

[7] Ford S, Despeisse M. Additive manufacturing and sustainability: an exploratory study of the advantages and challenges [J]. Journal of Cleaner Production, 2016, **137:** 1573-1587.

[8] Baumers M, Tuck C, Bourell DL, Sreenivasan R, Hague R. Sustainability of additive

manufacturing: measuring the energy consumption of the laser sintering process [J]. Proceedings of the Institution of Mechanical Engineers, Part B: Journal of Engineering Manufacture, 2011, **225**(12)**:** 2228-2239.

[9] Telenko C, Seepersad CC. A comparison of the energy efficiency of selective laser sintering and injection molding of nylon parts [J]. Rapid Prototyping Journal, 2012, **18**(6)**:** 472-481.

[10] Zhu Y, Peng T, Jia G, Zhang H, Xu S, Yang H. Electrical energy consumption and mechanical properties of selective-laser-melting-produced 316L stainless steel samples using various processing parameters [J]. Journal of cleaner production, 2019, **208:** 77-85.

[11] Song R, Telenko C. Material and energy loss due to human and machine error in commercial FDM printers [J]. Journal of Cleaner Production, 2017, **148:** 895-904.

[12] Peng T, Yan F. Dual-objective analysis for desktop FDM printers: energy consumption and surface roughness [J]. Procedia CIRP 2018, **69:** 106-111.

[13] Ajay J, Song C, Rathore AS, Zhou C, Xu W. 3DGates: an instruction-level energy analysis and optimization of 3D printers [J]. ACM SIGPLAN Notices, 2017, **52**(4)**:** 419-433.

[14] Peng T. Analysis of energy utilization in 3d printing processes. Procedia Cirp 2016, **40:** 62-67.

[15] Meteyer S, Xu X, Perry N, Zhao YF. Energy and Material Flow Analysis of Binder-jetting Additive Manufacturing Processes [J]. Procedia CIRP, 2014, **15:** 19-25.

[16] Hettesheimer T, Hirzel S, Ro? HB. Energy savings through additive manufacturing: an analysis of selective laser sintering for automotive and aircraft components [J]. Energy Efficiency, 2018, **11**(5)**:** 1227-1245.

[17] Xu X, Meteyer S, Perry N, Zhao YF. Energy consumption model of Binder-jetting additive

manufacturing processes [J]. International Journal of Production Research, 2015, **53**(23)**:** 7005-7015.

[18] Paul R, Anand S. Process energy analysis and optimization in selective laser sintering [J]. Journal of Manufacturing Systems, 2012, **31**(4)**:** 429-437.

[19] Ma F, Zhang H, Hon K, Gong Q. An optimization approach of selective laser sintering considering energy consumption and material cost [J]. Journal of Cleaner Production, 2018, **199:** 529-537.

[20] Huang R, Riddle M, Graziano D, Warren J, Das S, Nimbalkar S, Cresko J, Masanet E. Energy and emissions saving potential of additive manufacturing: the case of lightweight aircraft components [J]. Journal of Cleaner Production, 2016, **135:** 1559-1570.

[21] Kellens K, Mertens R, Paraskevas D, Dewulf W, Duflou JR. Environmental Impact of Additive Manufacturing Processes: Does AM contribute to a more sustainable way of part manufacturing? [J]. Procedia CIRP, 2017, **61:** 582-587.

[22] Le Bourhis F, Kerbrat O, Dembinski L, Hascoët J-Y, Mognol P. Predictive model for environmental assessment in additive manufacturing process [J]. Procedia CIRP, 2014, **15:** 26-31.

[23] Li Y, Linke BS, Voet H, Falk Br, Schmitt R, Lam M. Cost, sustainability and surface roughness quality – A comprehensive analysis of products made with personal 3D printers [J]. CIRP Journal of Manufacturing Science & Technology, 2017, **16:** 1-11.

[24] Kellens K, Renaldi R, Dewulf W, Kruth J-p, Duflou JR. Environmental impact modeling of selective laser sintering processes [J]. Rapid Prototyping Journal, 2014, **20**(6)**:** 459-470.

[25] Rejeski D, Zhao F, Huang Y. Research needs and recommendations on environmental

682 implications of additive manufacturing [J]. Additive Manufacturing, 2018, **19:** 21-28.

683 [26] Peng T, Kellens K, Tang R, Chen C, Chen G. Sustainability of additive manufacturing: An

684 overview on its energy demand and environmental impact [J]. Additive Manufacturing, 2018,

685 **21:** 694-704.

686 [27] Lei Zhang, Beikun Zhang, Hong Bao, Cheng Zhang, Weiwei Zhang. Carbon Emissions

687 Quantitative Methodology of Product Fused Deposition Manufacturing [J]. Chinese Journal

688 of Mechanical Engineering, 2017, 53(5):50-59.

689 [28] Medellin-Castillo HI, Zaragoza-Siqueiros J. Design and Manufacturing Strategies for Fused

690 Deposition Modelling in Additive Manufacturing: A Review [J]. Chinese Journal of

691 Mechanical Engineering, 2020(3)**:** 13-28.

692

Figures

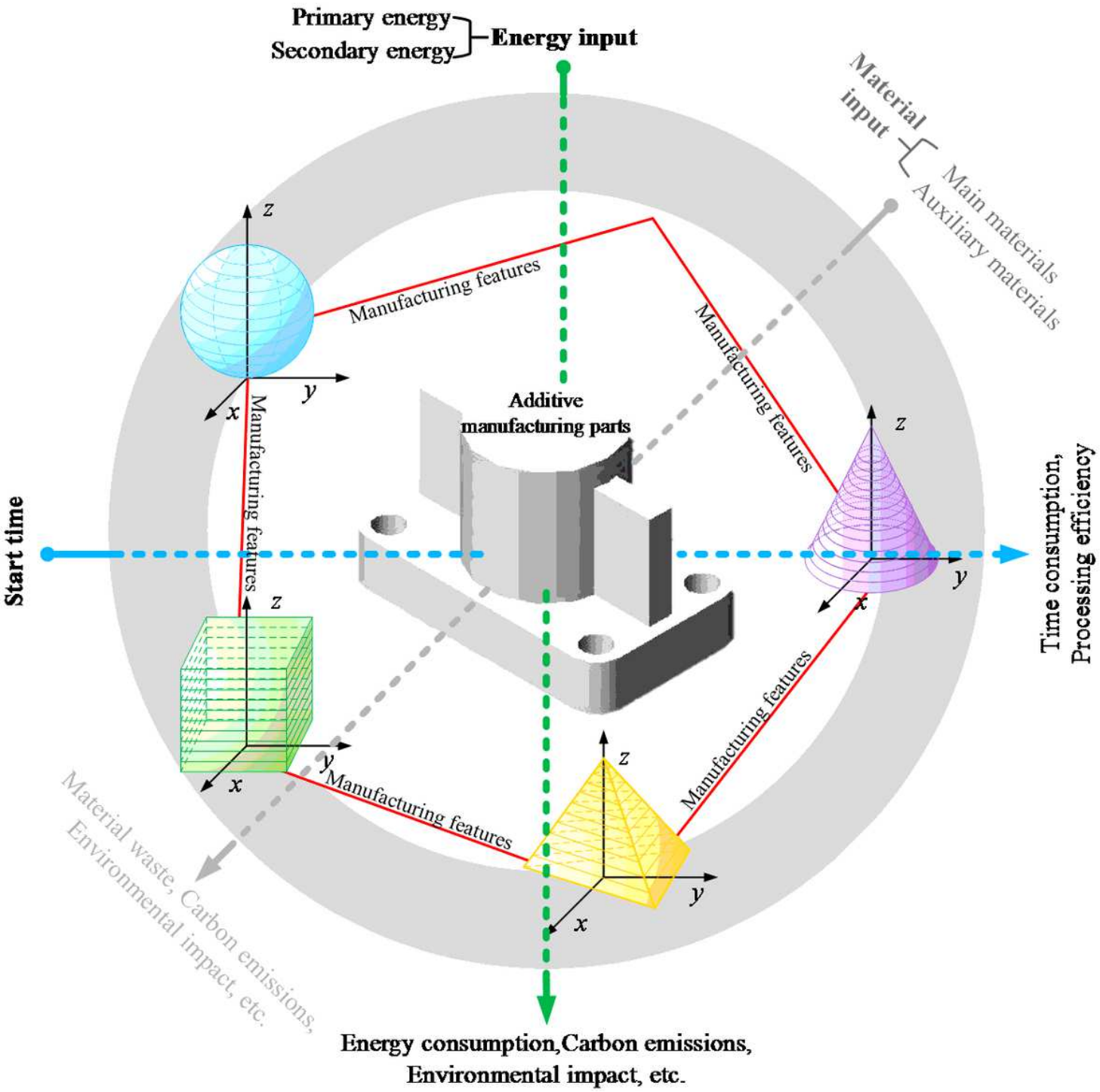

Figure 1

System boundary of feature-based energy consumption analysis of additive manufacturing (AM) parts

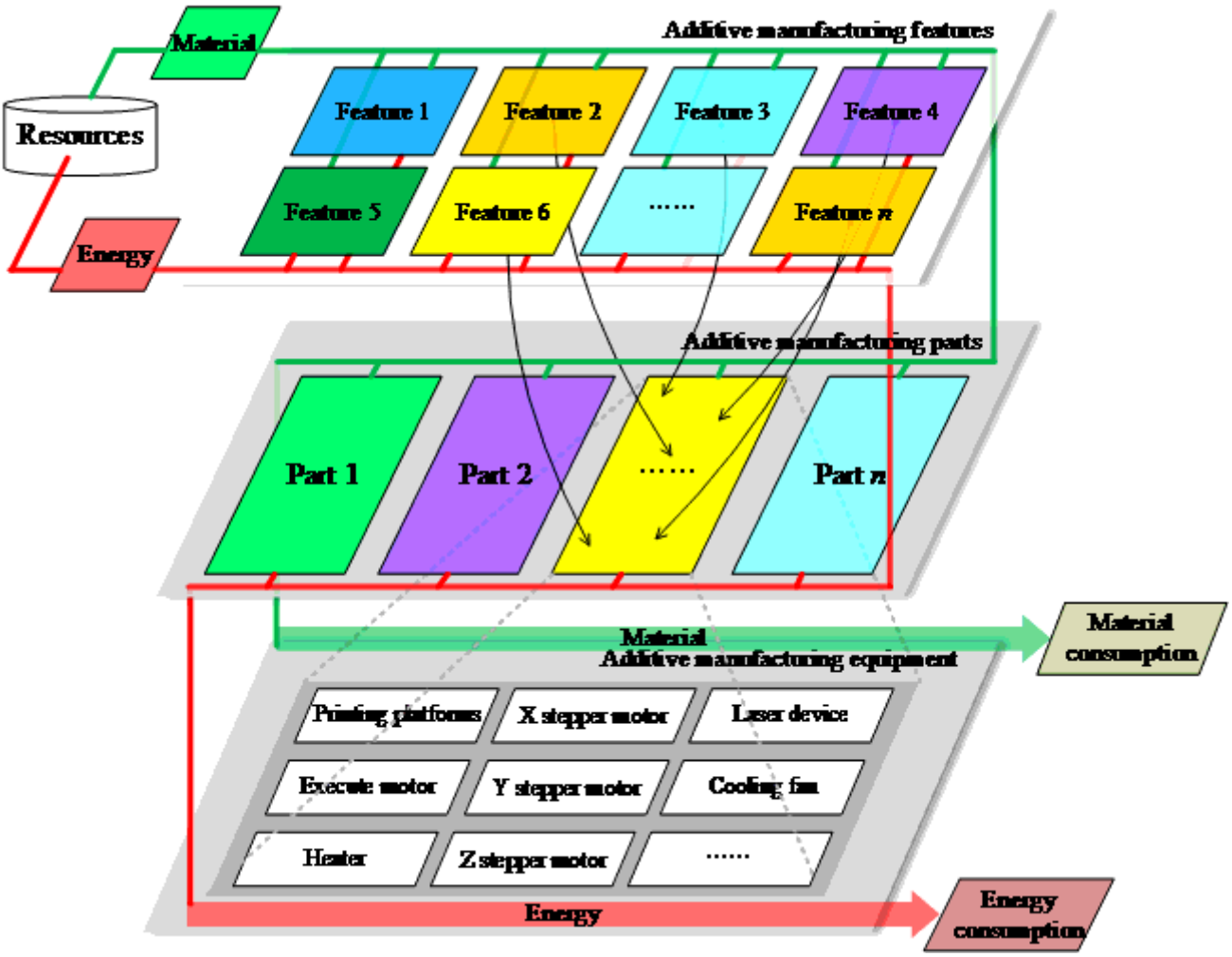

Figure 2

Schematic view and features of additive manufacturing (AM) system hierarchy

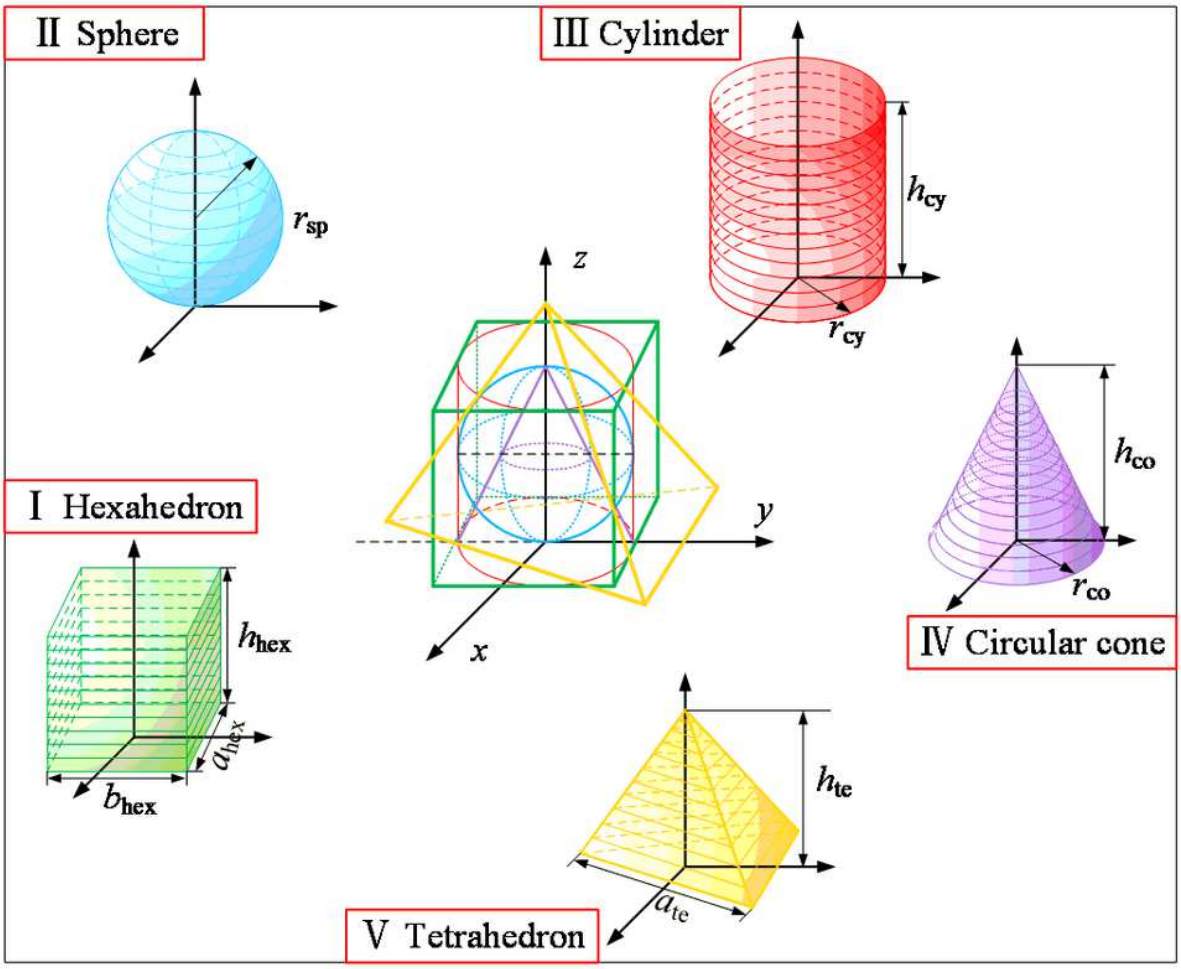

Figure 3

Typical additive manufacturing features (AMFs) and their related parameters

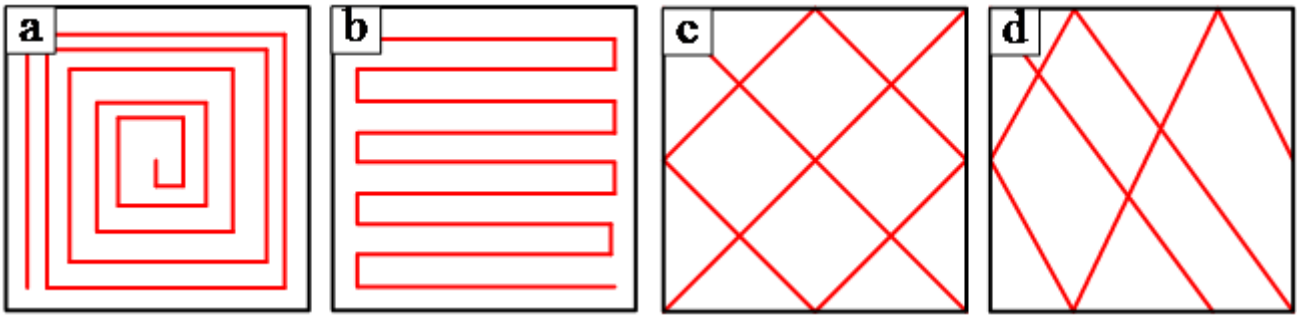

Figure 4

Different object in-fill patterns: (a) Square-circle; (b) Line; (c) Grid; (d) Triangle

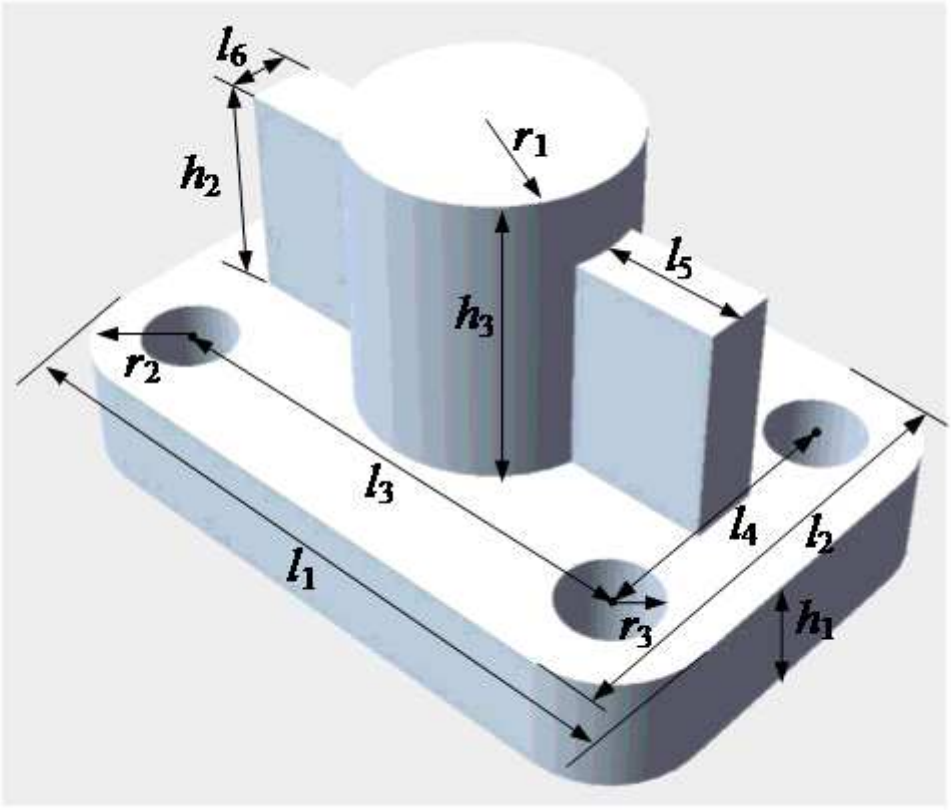

Figure 5

Computer-aided design (CAD) model of the processed additive manufacturing (AM) parts

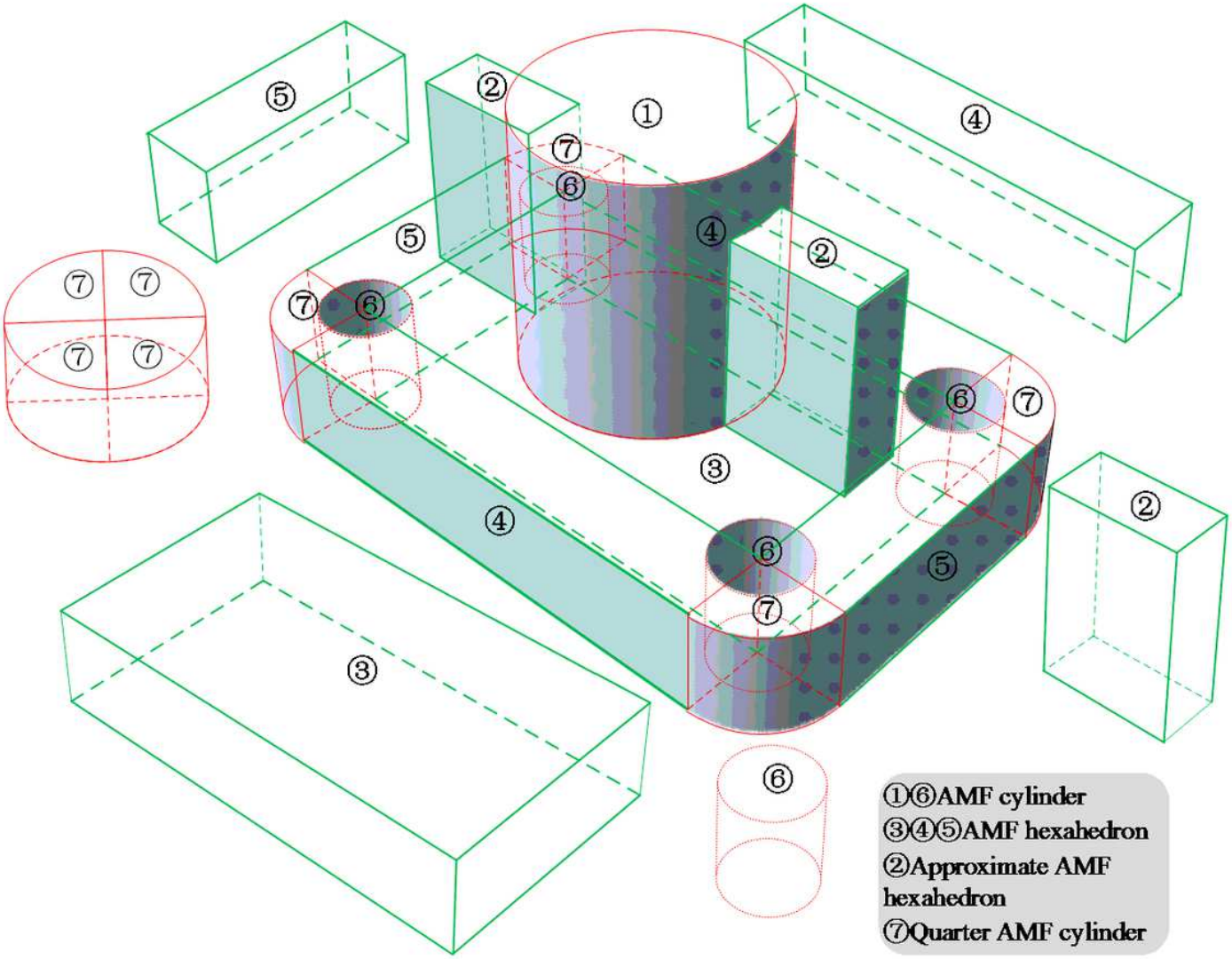

Figure 6

Manufacturing feature segmentation of processed additive manufacturing (AM) parts

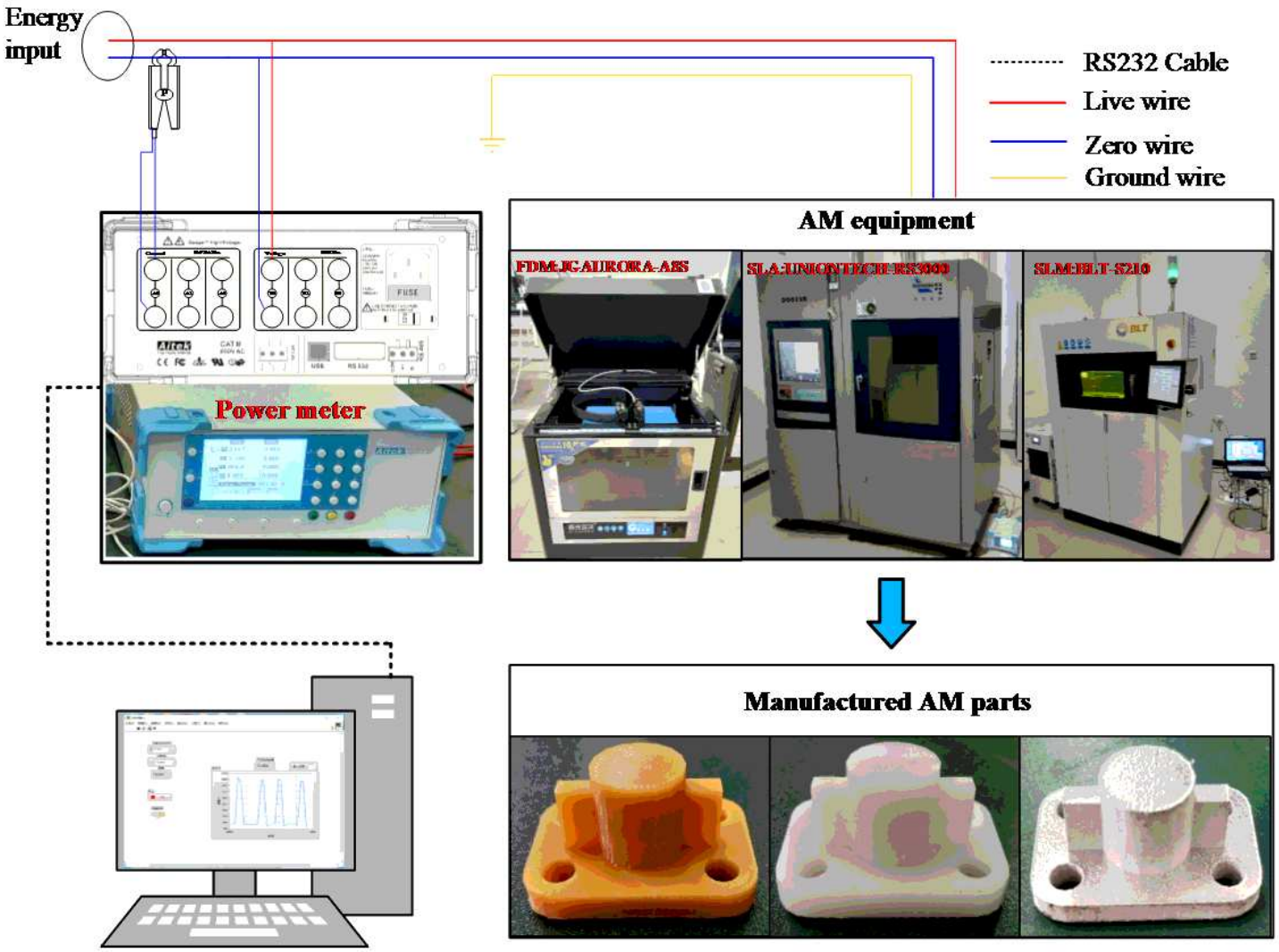

Figure 7

Schematic of the experimental testing system

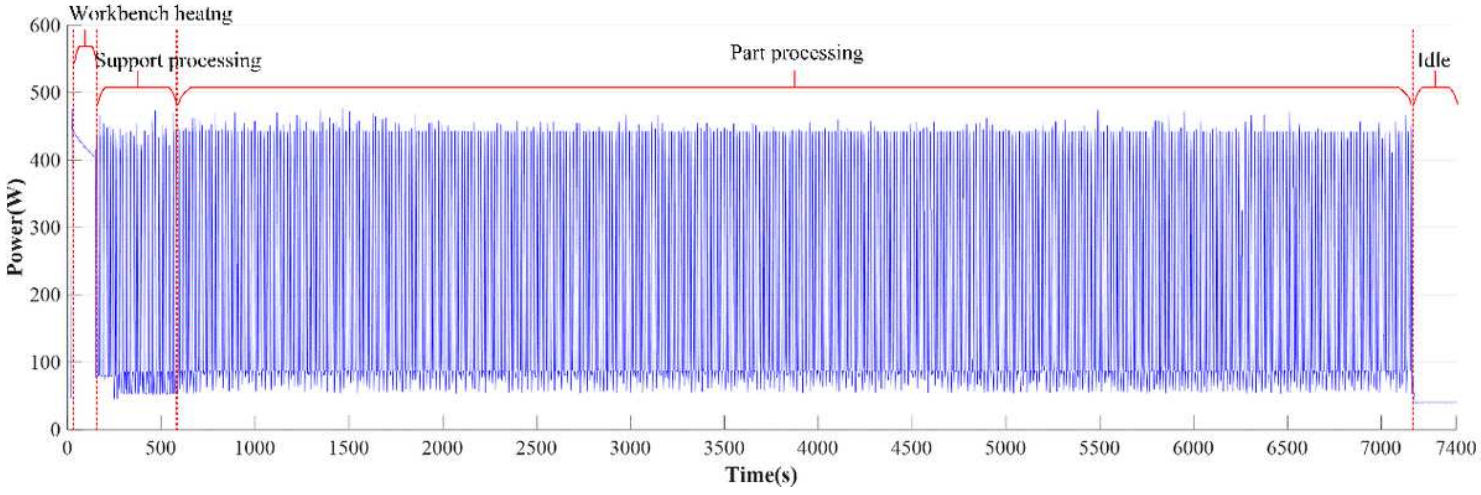

Figure 8

Power consumption vs time for an entire FDM process

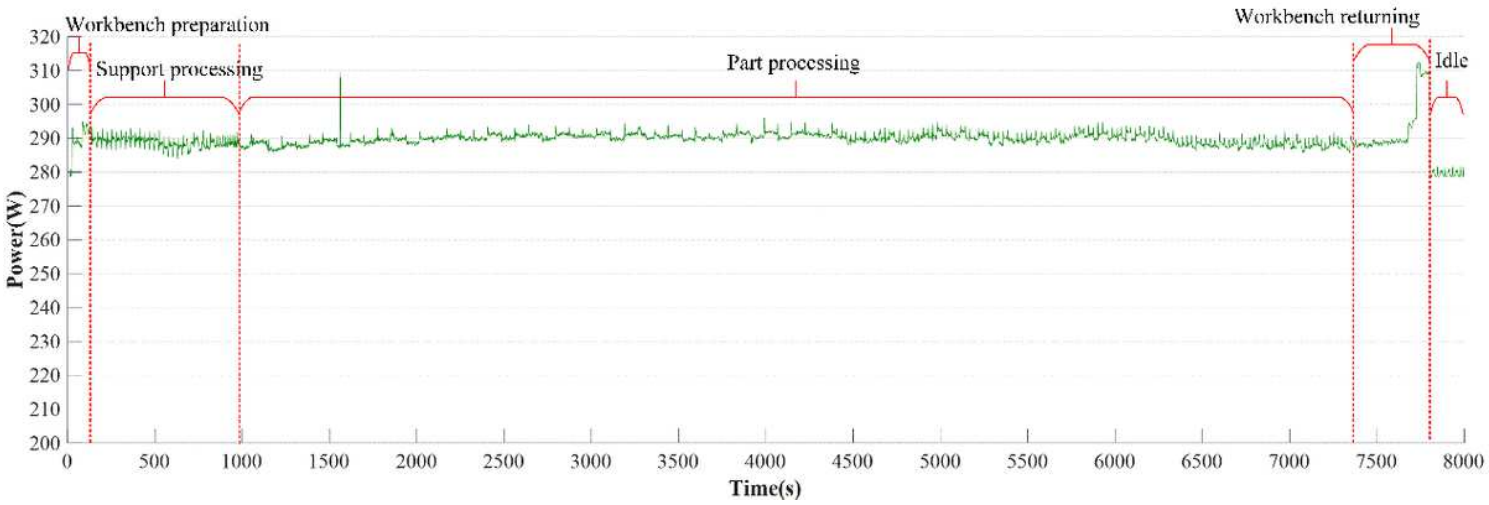

Figure 9

Power consumption vs time for an entire SLA process

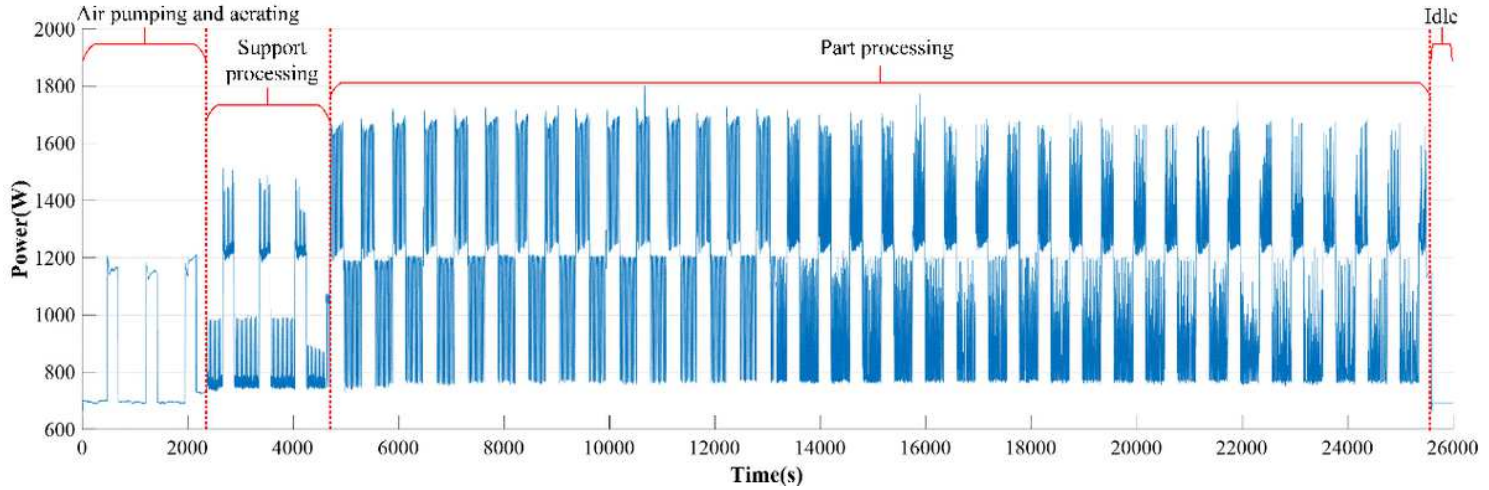

Figure 10

Power consumption vs time for an entire SLM process

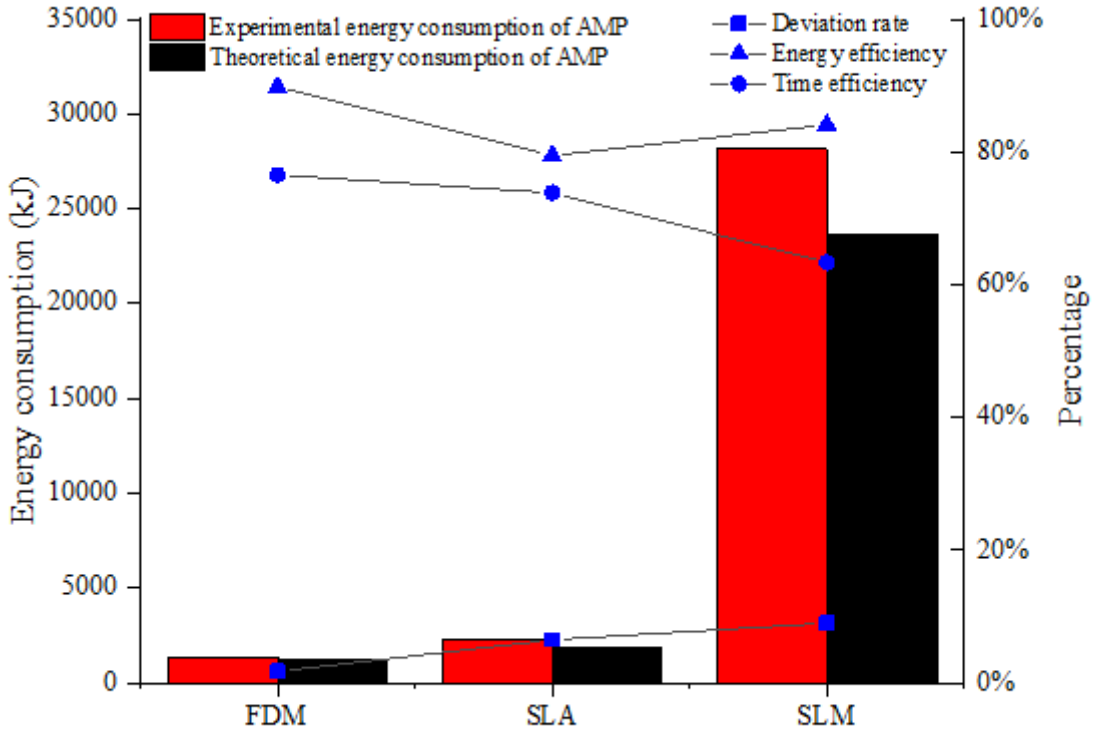

Figure 11

Energy consumption and efficiency indicators comparison under different AM technologies

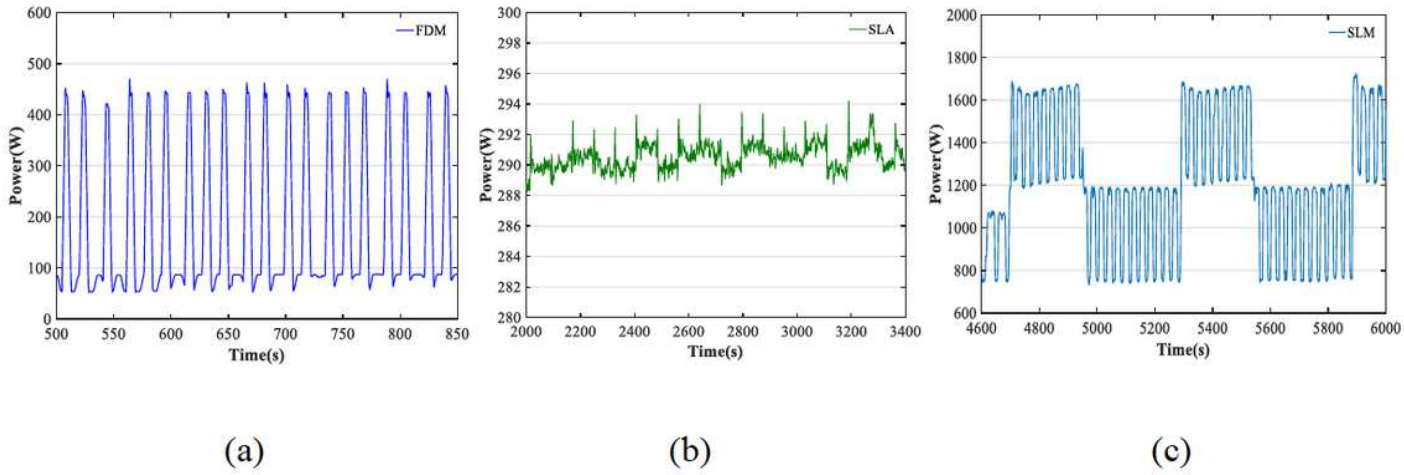

Figure 12

Zoomed-in section of power during the forming stage: (a) FDM process, (b) SLA process, (c) SLM process